

2P  
m 11

# GOODYEAR AEROSPACE

GOODYEAR AEROSPACE CORPORATION

GOODYEAR AEROSPACE CORPORATION

GOODYEAR AEROSPACE CORPORATION

(NASA-CR-124073) STUDY OF LARGE FLEXIBLE  
TUNNEL FOR SHUTTLE/PAYLOAD INTERFACE  
(Goodyear Aerospace Corp.) 79 p HC  
\$6.00

N73-17879

CSCL 22B

Unclas

G3/31 17197

Reproduced by  
NATIONAL TECHNICAL  
INFORMATION SERVICE  
US Department of Commerce  
Springfield, VA. 22151

# GOODYEAR AEROSPACE CORPORATION

AKRON, OHIO 44315

STUDY OF  
LARGE FLEXIBLE TUNNEL  
FOR  
SHUTTLE/PAYLOAD INTERFACE

GER-15834

22 November 1972

E-ID-26(7-71)  
REF: EOI 380

Details of illustrations in  
this document may be better  
studied on microfiche

## FOREWORD

This document was prepared by Goodyear Aerospace Corporation, Akron, Ohio under Contract NAS 8-28951 with George C. Marshall Space Flight Center. R. Crumbley, S & E-ASTN-ESD, was the NASA Project Engineer.

This report covers work that was started in June 1972 and completed in November 1972. J. W. Haylett of the Aero-Mechanical Systems Division was the Goodyear Aerospace Project Engineer.

The work was accomplished as a cooperative effort by personnel from the various specialties listed as follows:

Concept Design and Development  
Structural Analysis  
Environmental Analysis  
Materials  
Contract Administration

N. D. Brown  
G. L. Jeppesen  
W. W. Sowa  
K. L. Cordier  
C. H. Secaur

# TABLE OF CONTENTS

Section		Page
I	INTRODUCTION. . . . .	1
II	STATEMENT OF REQUIREMENT. . . . .	6
	A. Requirements. . . . .	6
	1. Thermal . . . . .	6
	2. Pressure. . . . .	6
	3. Load Criteria . . . . .	6
	4. Acoustic Criteria . . . . .	7
	5. Meteoroid Flux. . . . .	7
	6. Altitude. . . . .	7
	7. Tunnel Geometry . . . . .	7
	B. Guidelines. . . . .	7
	1. Materials . . . . .	7
	C. Objectives. . . . .	7
III	PRELIMINARY STUDY . . . . .	9
	A. General . . . . .	9
	B. Tunnel Configuration. . . . .	9
	1. Configuration A Truncated Spheres . . . . .	9
	2. Configuration B Truncated Cones . . . . .	9
	3. Configuration C Helical Spring. . . . .	12
	4. Configuration D Ring Supported Tunnel . . . . .	12
	5. Configuration E Cable Supported Tunnel. . . . .	12
	C. Preliminary Study Summary . . . . .	16
	1. Configurations A and B Truncated Cones and Spheres . . . . .	16
	2. Configuration C Helical Spring. . . . .	16
	3. Configuration D Ring Supported Tunnel . . . . .	16
	4. Configuration E Cable Supported Tunnel. . . . .	16
	D. Cable Supported Tunnel Model. . . . .	16
IV	SELECTED CONFIGURATION. . . . .	19
	A. General . . . . .	19
	B. Full-Scale Model. . . . .	19
	C. Structural Analysis . . . . .	23
	1. General . . . . .	23
	2. Analysis Summary. . . . .	23
	D. Material Selection (Expandable Structure) . . . . .	24
	1. General . . . . .	24
	2. Outer Cover Layer . . . . .	24
	3. Structural Layer. . . . .	24
	4. Micrometeoroid Layer. . . . .	24

Section	Page
5. Pressure Bladder . . . . .	28
6. Composite Fabric Weight . . . . .	28
7. Environmental Compatibility . . . . .	30
E. Micrometeoroid Analysis . . . . .	30
1. General . . . . .	30
2. Micrometeoroid Environment. . . . .	33
3. Probability of Impact . . . . .	34
4. Meteoroid Mass Calculation. . . . .	35
5. Micrometeoroid Shield Thickness . . . . .	36
F. Thermal Properties of Tunnel Wall . . . . .	38
1. Tunnel Wall Configuration . . . . .	38
2. Thermal Properties of Tunnel Wall Material. . .	40
G. Weight Estimate . . . . .	40
V CONCLUSIONS AND RECOMMENDATIONS . . . . .	43
Appendix	
I STRUCTURAL ANALYSIS . . . . .	45

# LIST OF ILLUSTRATIONS

Figure		Page
1	Shuttle/Payload Interface Tunnel Model - Straight Deployment. . . . .	2
2	Shuttle/Payload Interface Tunnel Model - Curved Deployment. . . . .	3
3	Shuttle/Payload Interface Tunnel Model - Internal Views	4
4	Tunnel Geometry . . . . .	8
5	Configuration A Truncated Spheres . . . . .	10
6	Configuration B Truncated Cones . . . . .	11
7	Configuration C Helical Spring. . . . .	13
8	Configuration D Ring Supported Tunnel . . . . .	14
9	Configuration E Cable Supported Tunnel. . . . .	15
10	Cable Diagram . . . . .	18
11	Envelope Dimensions . . . . .	20
12	Existing Technology . . . . .	25
13	Elastic Recovery Materials Technique. . . . .	26
14	Outer Cover . . . . .	26
15	Foam Thickness Recovery Versus Time . . . . .	29
16	Pressure Bladder. . . . .	30
17	Schematic of Micrometeoroid Hazard to Tunnel. . . . .	32
18	Foam Thickness vs Projectile Weight V <sub>p</sub> 6 KM/SEC. . . . .	37
19	Schematic of Tunnel Wall Materials. . . . .	39

# LIST OF TABLES

Table		Page
I	Preliminary Study Results . . . . .	17
II	Fiber B Woven Cloth Specification Summary . . . . .	27
III	Unit Weight Breakdown . . . . .	28
IV	Environmental Compatibility - Expandable Material . . . .	31
V	Thermal Properties of Wall Materials. . . . .	41
VI	Estimated Weight Breakdown. . . . .	42

## SECTION I

### INTRODUCTION

Goodyear Aerospace Corporation (GAC) has conducted a five-month theoretical and preliminary design study of a large flexible tunnel for use at the shuttle/payload interface. The theoretical study consisted of evaluating various design concepts and determining their adaptability to the tunnel requirements. The theoretical study culminated in the selection of one concept. The selected concept was documented with preliminary drawings of a full-scale ground test model. Supporting preliminary structural, thermal, micrometeoroid, material, and weight analyses were conducted.

The specified tunnel requirements could be broadly grouped into two categories; i.e., environmental and performance. The environmental requirements were those ambient conditions and loads associated with ground, launch, space and reentry of the shuttle vehicle. Materials are presently available which will meet all these environmental requirements and can be designed into the structure to withstand the specified loads. The material state-of-the-art can, however, be significantly extended by using a new material, Fiber B, developed by DuPont and presently being utilized in a GAC program on the B-1 aircraft. This Fiber B material has significant advantages in strength-to-weight ratios and flexibility when compared to other metal, natural, or synthetic fibers. This new fiber was considered in the tunnel flexible structure.

The performance requirements proved to be the most challenging aspect of the program and required the development of a new deployment concept. The specific condition requiring the tunnel development was the ability to deploy pressurized either straight or curved in an arc of about 90 degrees, and also to deploy pressurized to any straight length from packaged length to fully deployed length. Other performance requirements such as deployment cycles, leak rate, etc., proved to be only minor problems and are considered to be within existing state-of-the-art.

The systematic approach used on the program to select a design configuration included a theoretical study evaluating all concepts that appeared feasible. From this study, one concept, identified as the cable-supported tunnel, was selected as the configuration which best met the total system requirements. To verify the characteristics of this concept, a one-fourth scale model was fabricated (see Figures 1, 2 and 3). As a result of the satisfactory functional tests on this model, GAC and MSFC mutually selected the cable-supported tunnel as the prime concept. Other concepts considered and eliminated included truncated spheres, truncated cones, helical spring-supported tunnel, and ring-supported tunnel.

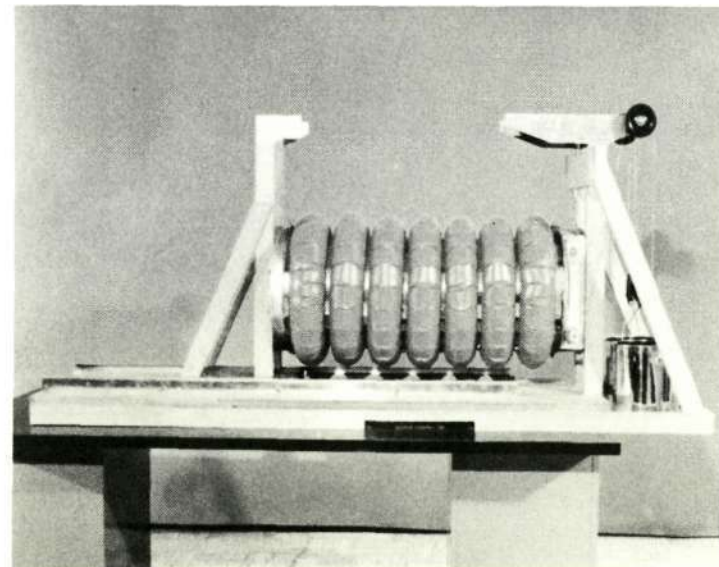
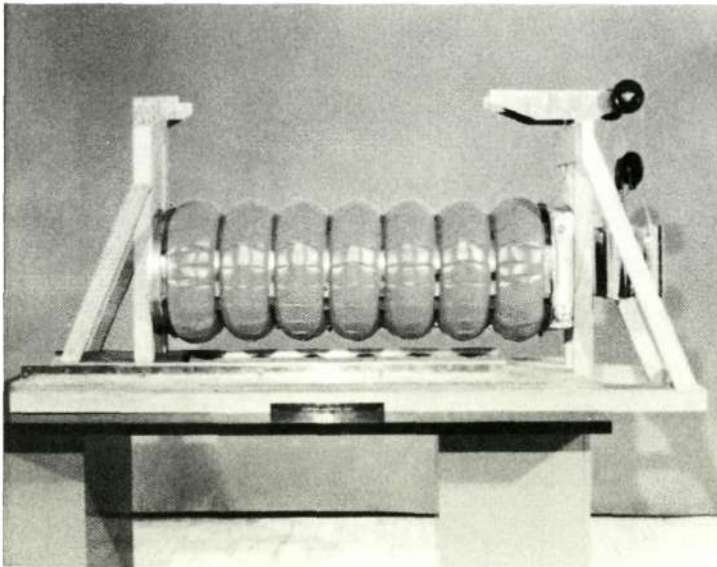
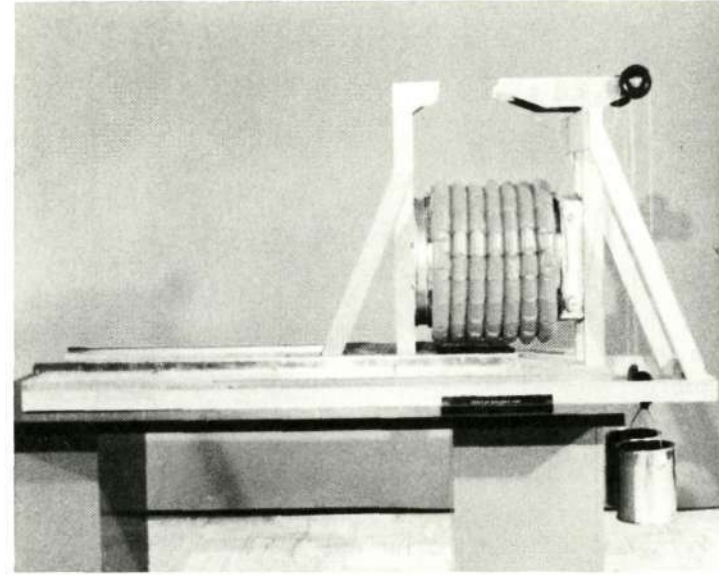
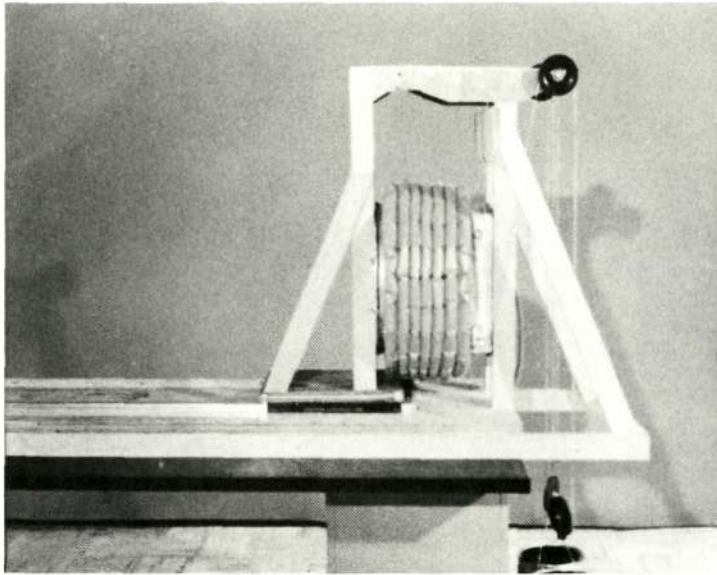


Figure 1. Shuttle/Payload Interface Tunnel Model - Straight Deployment

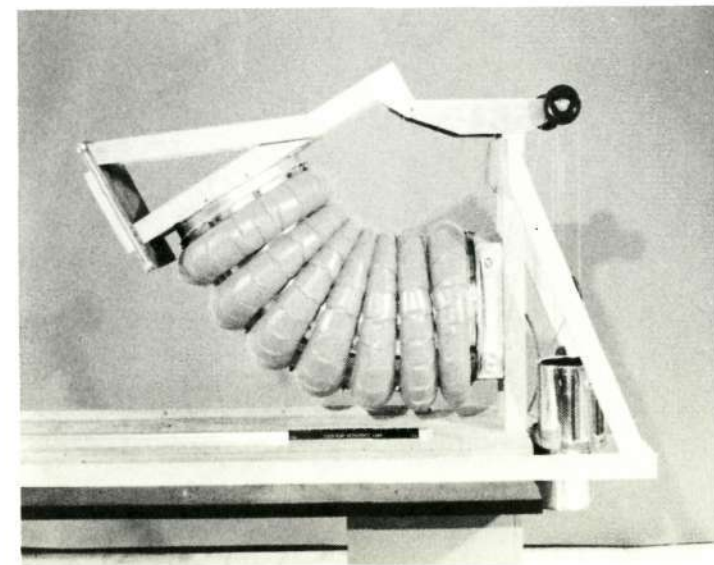
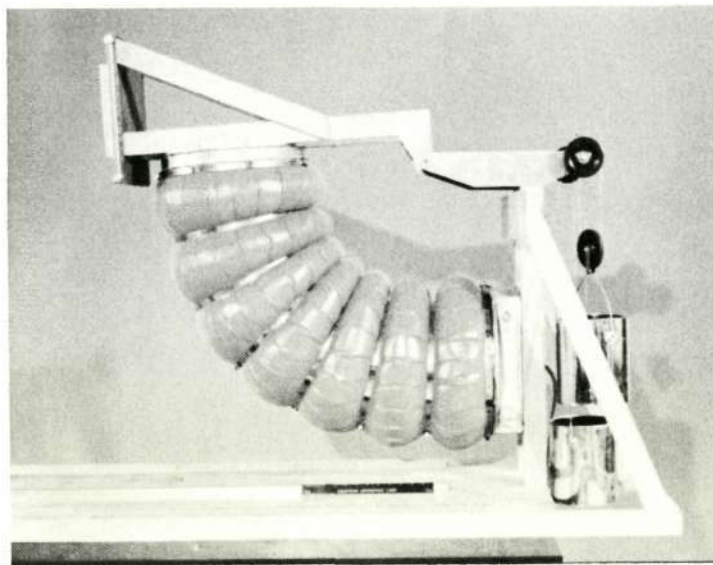
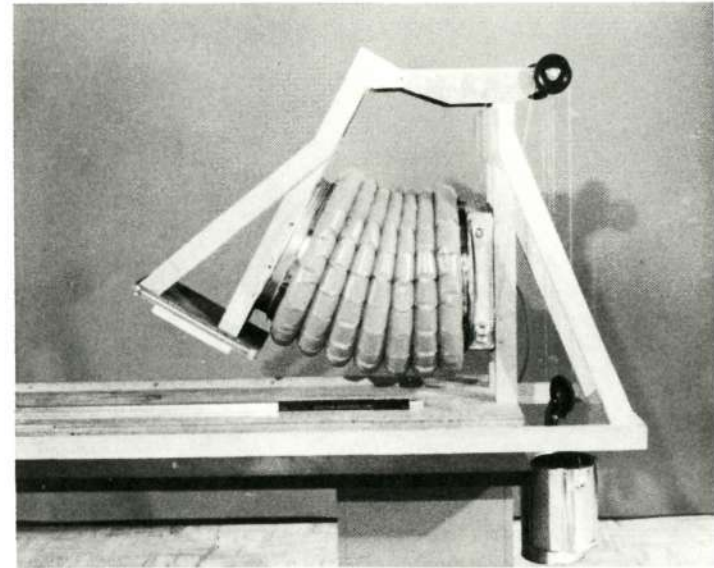
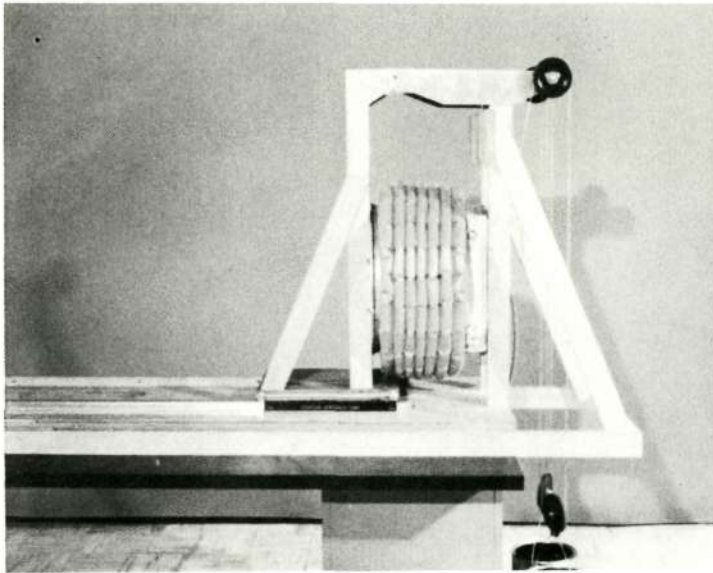


Figure 2. Shuttle/Payload Interface Tunnel Model - Curved Deployment

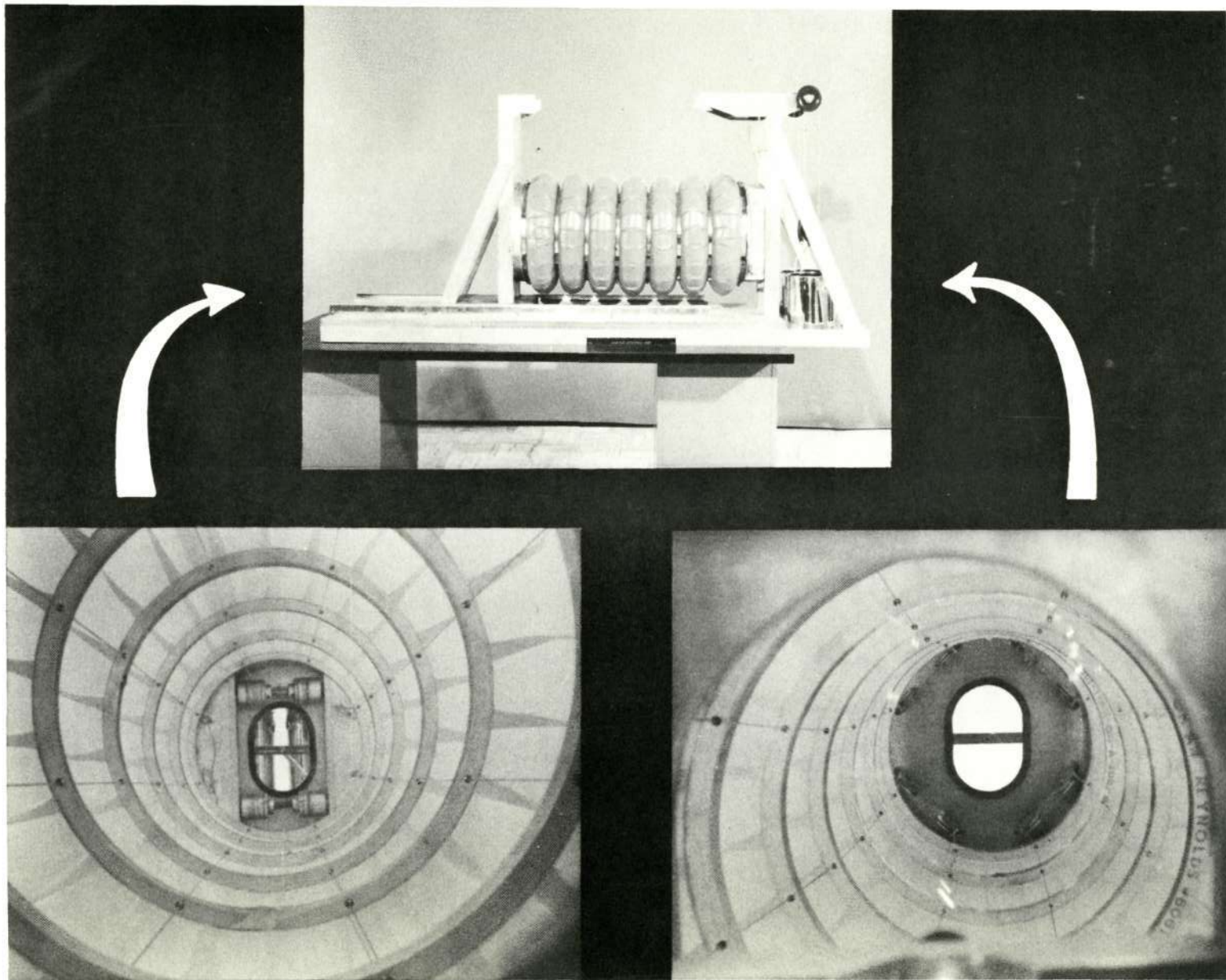


Figure 3. Shuttle/Payload Interface Tunnel Model - Internal Views

Preliminary drawings of a full-scale ground test model of the cable-supported tunnel were completed. The flexible components of the tunnel will be fabricated of material suitable for ultimate shuttle application. The metal parts, such as tunnel rings, cables, pulleys, pulley supports, interface rings, and bulkheads, were designed utilizing the most economical materials and fabrication methods. With this philosophy, the maximum amount of data can be obtained on the tunnel at minimum cost. Preliminary supporting analysis of the ground-test model was also completed in sufficient detail to demonstrate the feasibility of the concept, and also to estimate the weight of the component parts. The weight breakdown includes the weight of the ground-test model and the projected weight if designed for the space shuttle application.

## SECTION II

### STATEMENT OF REQUIREMENT

The development and design of the flexible tunnel considered the following requirements, guidelines, and objectives:

#### A. REQUIREMENTS

##### 1. Thermal

<u>Condition</u>	<u>Temperature Range</u>
Astronaut Touch Temperature	276°K to 313°K (+38°F to +105°F)
Prelaunch	277°K to 321°K (+40°F to +120°F)
Launch	277°K to 338°K (+40°F to +150°F)
Orbit - Bay Doors Closed	199°K to 338°K (-100°F to +150°F)
Orbit - Bay Doors Open	199°K to 388°K (-100°F to +150°F)
Entry	199°K to 366°K (-100°F to +200°F)

##### 2. Pressure

Maximum internal gage pressure  $1.027 \times 10^5 \text{ N/m}^2$  (14.7  $\pm$  0.2 psi)

##### 3. Load Criteria

Condition	G Loads						Tunnel Pressure Differential
	X		Y		Z		
	Max	Min	Max	Min	Max	Min	
1. Orbit Abort	+2.5	-4.5	+1.0	-1.0	+1.2	-1.2	Min
2. Re-Entry	+1.4	+0.6	+0.7	-0.7	+4.0	+2.0	$1.01 \times 10^5 \text{ N/m}^2$ (14.7 $\pm$ 0.2)
3. Module Deployment	+0.2	-0.2	+0.2	-0.2	+0.2	-0.2	$1.01 \times 10^5 \text{ N/m}^2$ (14.7 $\pm$ 0.2)
4. Crash Landing	+1.5	-8.0	+1.5	-1.5	+2.0	-4.5	Min

### Notes

Apply F.S. of 3 to conditions 1, 2, and 3.

G loads given for crash condition are ultimate.

In design use worst possible combination of G loads for any condition.

+X axis is longitudinal to the rear.

+Y axis is transverse to the right looking forward.

+Z axis is up.

#### 4. Acoustic Criteria

Not to exceed 145 db

#### 5. Meteoroid Flux

Refer to NASA TM X64627, November, 1971

#### 6. Altitude

Sea level to  $8.32 \times 10^5$  meters (450 nautical miles)

#### 7. Tunnel Geometry

The tunnel geometry shall be as depicted in Figure 4.

### B. GUIDELINES

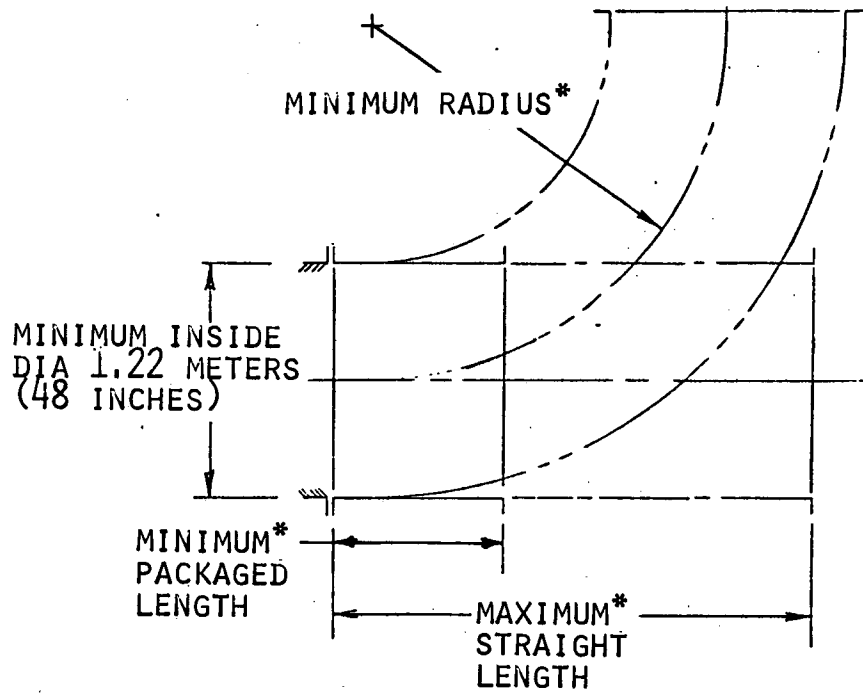
#### 1. Materials

All materials selected for use in habitable areas shall be nontoxic, nonflammable and nonexplosive to the maximum extent practicable.

### C. OBJECTIVES

The design shall be characterized by:

- (1) The ability to deploy as a straight or curved tunnel in an arc of about 90 degrees. The tunnel shall be stable at any deployed position from packaged to fully deployed.



\*TO BE DETERMINED DURING THE PROGRAM

Figure 4. Tunnel Geometry

- (2) Materials capable of withstanding the deployment cycles and launch, space, and re-entry environments.
- (3) Minimum leakage rate.
- (4) Minimum packaged length.
- (5) The ability to withstand  $1.01 \text{ N/m}^2$  (14.7 psi) internal pressure after deployment.
- (6) The ability to deploy and retract either pressurized or unpressurized.

### SECTION III

#### PRELIMINARY STUDY

##### A. GENERAL

The objective of the preliminary study was to qualitatively compare various flexible tunnel configurations and select the most promising concept for more detailed study. This effort, therefore, included evaluating both new and previously developed flexible materials as well as new and previously developed tunnel configuration concepts. Five tunnel concepts were selected for consideration, and the results of the evaluation is presented in matrix form.

##### B. TUNNEL CONFIGURATIONS

###### 1. Configuration A Truncated Spheres

The packaged, deployed straight and deployed curved pictorial arrangement is shown in Figure 5. The design consists of four filament-wound spherical segments bolted together at their apertures through aluminum frames. The frames are sealed with static O-ring seals. The two center spherical segments are identical and the two end segments are opposites. With an internal pressure of  $1.01 \text{ N/m}^2$  (14.7 psi) the tunnel has three structurally stable positions of packaged, deployed curved and deployed straight. To move the tunnel from the packaged to deployed position the internal gage pressure must be near zero. The tunnel can be configured on the ground to deploy either curved or straight by rotating alternate segments 180 degrees.

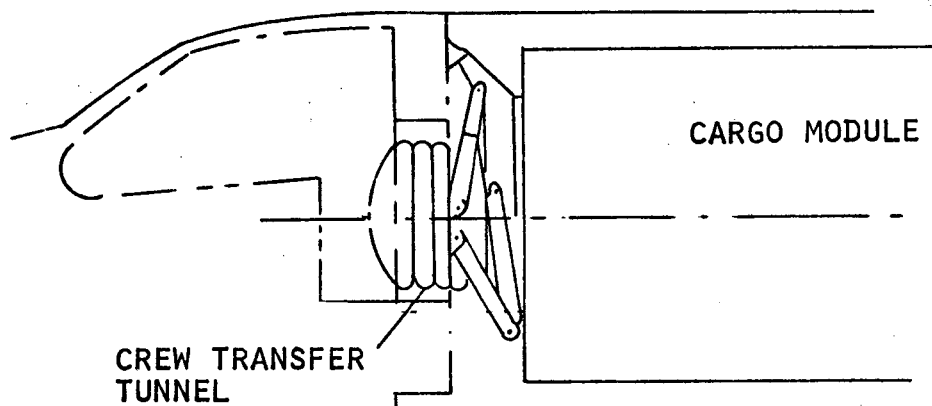
The tunnel wall would be a four layer composite of flexible material consisting of an inner pressure bladder, structural filament wound layer, micrometeoroid barrier and outer cover. Details of the material characteristics are discussed in Paragraph D of Section IV.

###### 2. Configuration B Truncated Cones

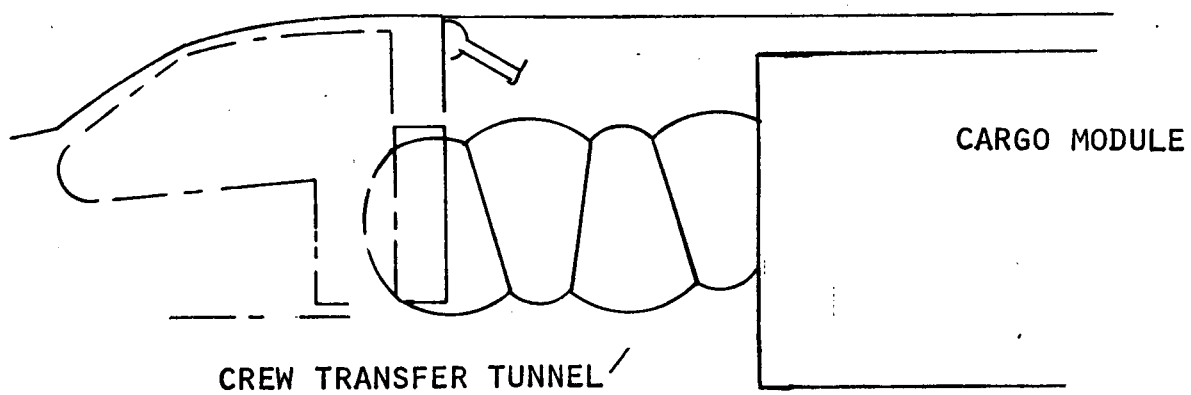
The packaged, deployed straight and deployed curved pictorial arrangement is shown in Figure 6. The design is essentially the same as the truncated spheres except the spheres are configured as cones to provide a smaller, more orderly packaging arrangement. The change from spheres to cones also requires the structural filament wound layer to be changed to a woven configuration. Either stainless steel or the new Fiber B material would be suitable fiber for the woven cloth.

The truncated cones have the same pressure, packaging and deployment limitations as the truncated sphere.

PACKAGED



DEPLOYED STRAIGHT



DEPLOYED CURVED

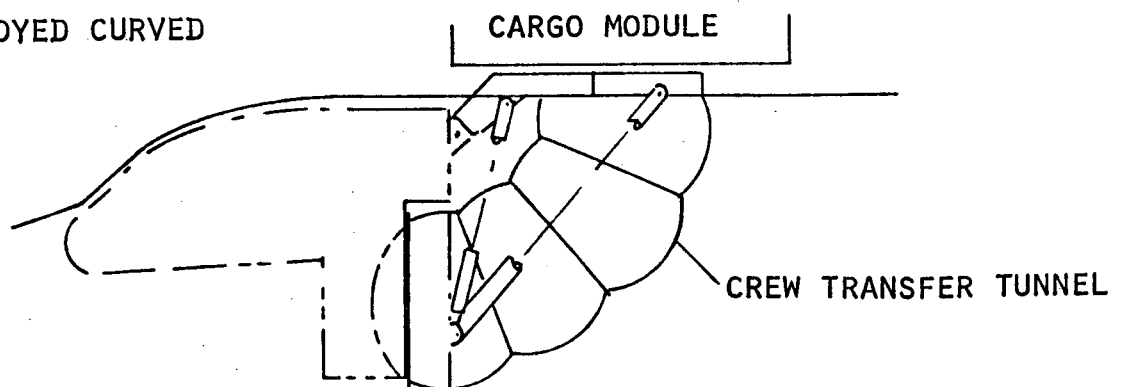
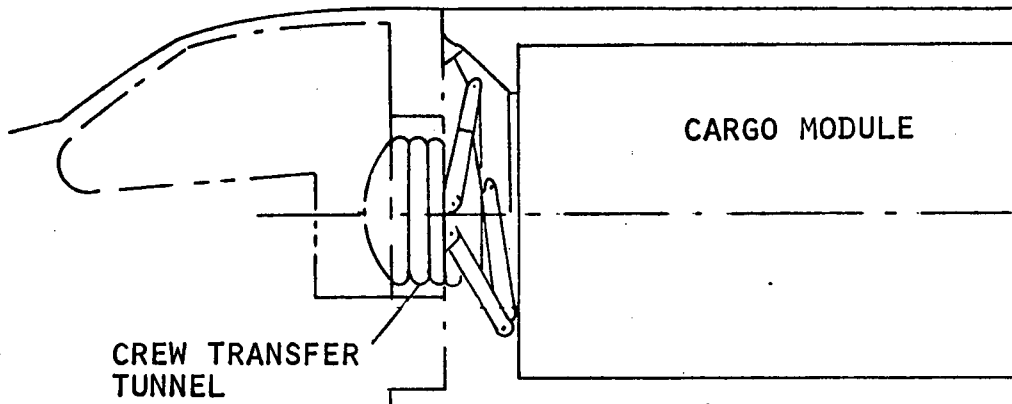


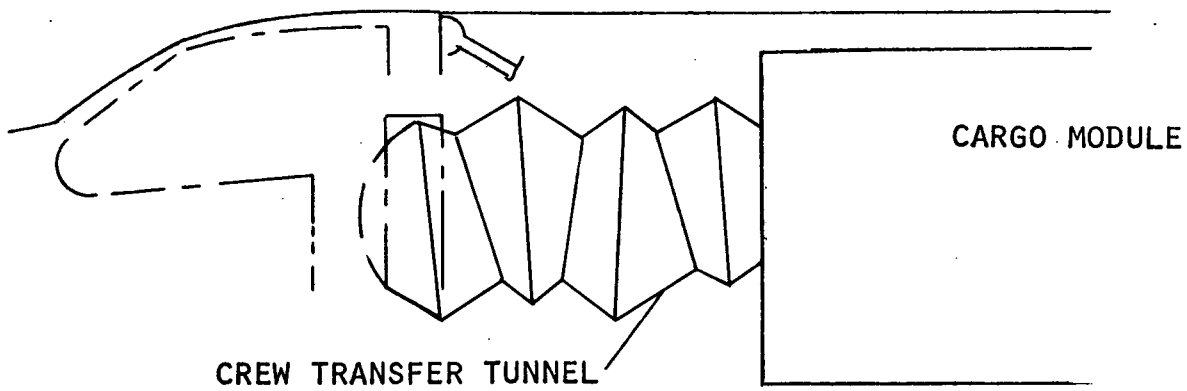
Figure 5. Configuration A Truncated Spheres

# SPACE SHUTTLE CREW TRANSFER TUNNEL

PACKAGED



DEPLOYED STRAIGHT



DEPLOYED CURVED

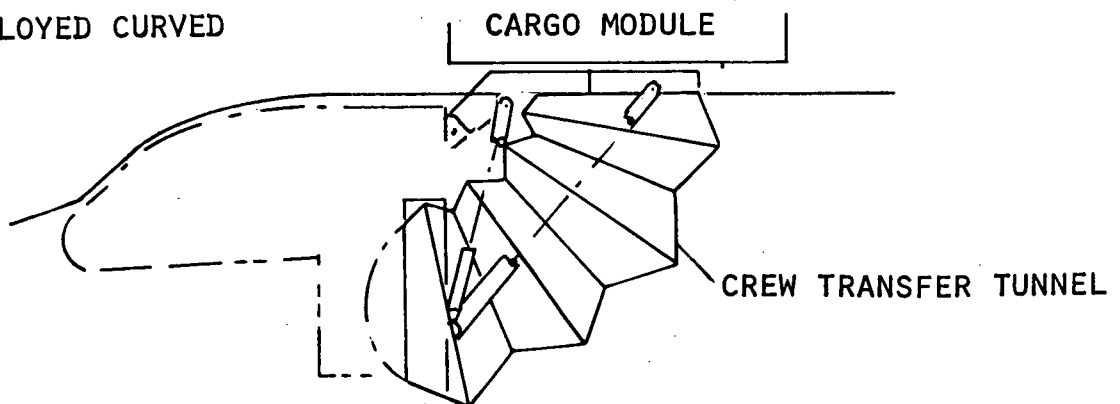


Figure 6. Configuration B Truncated Cones

### 3. Configuration C Helical Spring

The pictorial arrangement of this configuration is shown in Figure 7. The concept consists of a flexible structure pressure bladder encaged within a helical spring. Initially, it was believed that a spring structure could be designed which would permit controlled tunnel configurations during pressurized deployment from the package condition to either a straight length or curved position. In the preliminary analysis a realistic design did not appear feasible. It became evident during the analysis that spring weight would be excessive and the package length too long. The analysis was discontinued before completion in favor of more promising concepts.

### 4. Configuration D Ring Supported Tunnel

The pictorial arrangement of this configuration is shown in Figure 8. The concept consists of a flexible structure pressure bladder with rings equally spaced along the length of the tunnel. By controlling the transverse movement of the rings with either a hinge or guide rails the pressurized tunnel could be deployed either curved or straight. Axial spacing of the rings would be controlled by the lobes of the pressure bladder.

The tunnel wall would be a four-layer composite similar to the arrangement discussed in Paragraph D of Section IV.

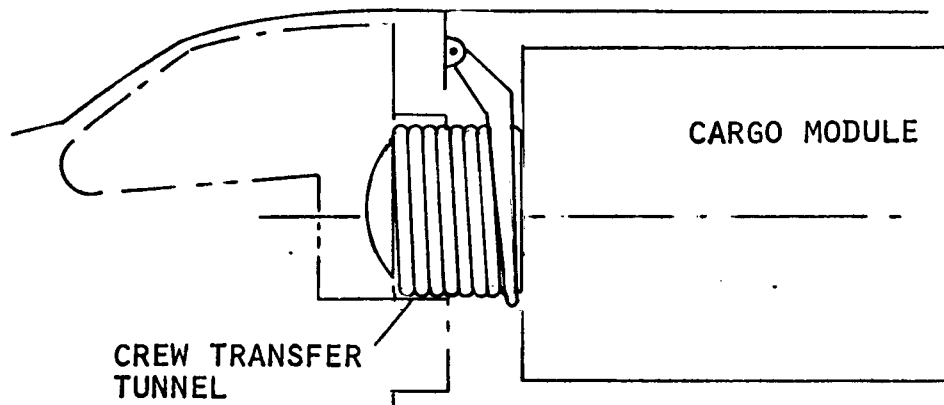
### 5. Configuration E Cable Supported Tunnel

The pictorial arrangement of this configuration is shown in Figure 9. The concept consists of a pressure bladder with rings equally spaced along the length of the tunnel. Transverse movement of the rings is limited by tension cables parallel to the axis of the tunnel and passing through the rings. The cables are equally spaced around the periphery of the tunnel. The rings are free floating axially on the cables and therefore will be equally spaced along the axis of the tunnel by the lobes of the pressure bladder.

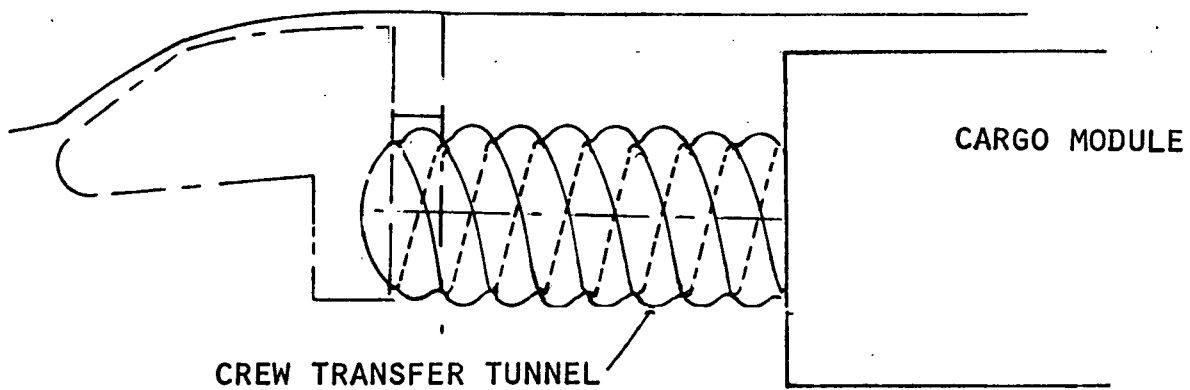
Deployment or retraction of the pressurized tunnel can be obtained by decreasing or increasing the tension in the cables. The curved or straight deployment is established by cargo module guides. The curved guide could be a hinge and the straight guide could be tracks or guides for the cargo module support points.

The tunnel wall would be four-layer composite similar to the arrangement discussed in Paragraph D of Section IV.

PACKAGED



DEPLOYED STRAIGHT



DEPLOYED CURVED

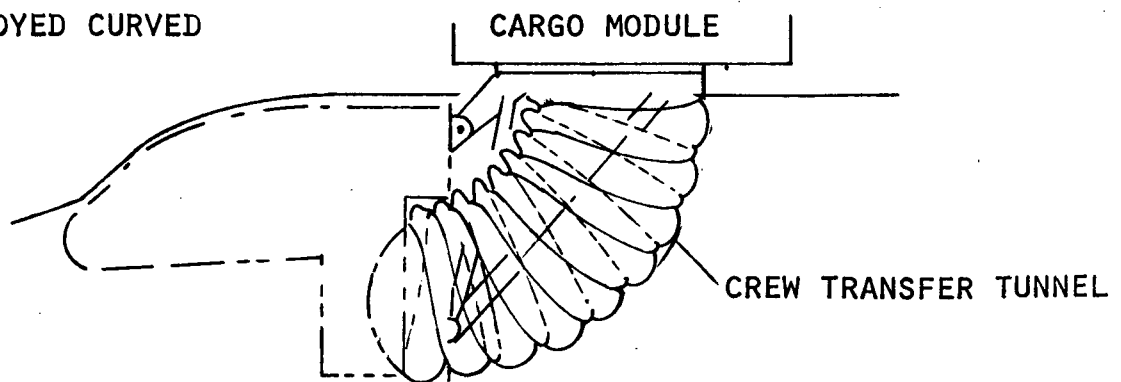
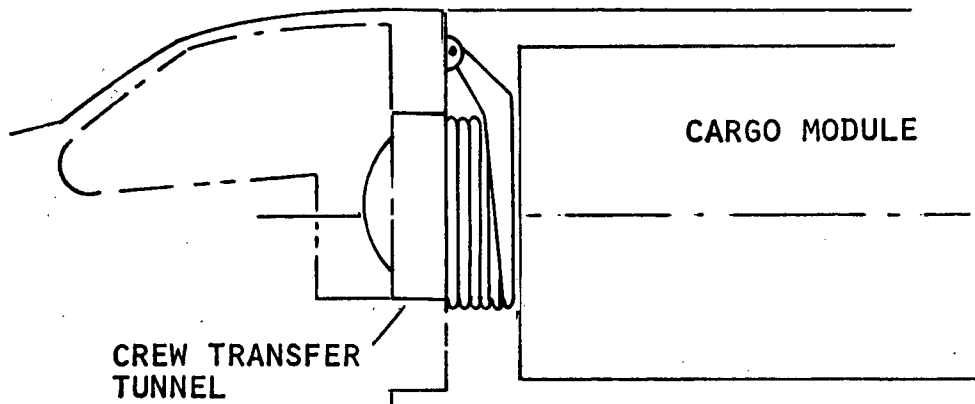
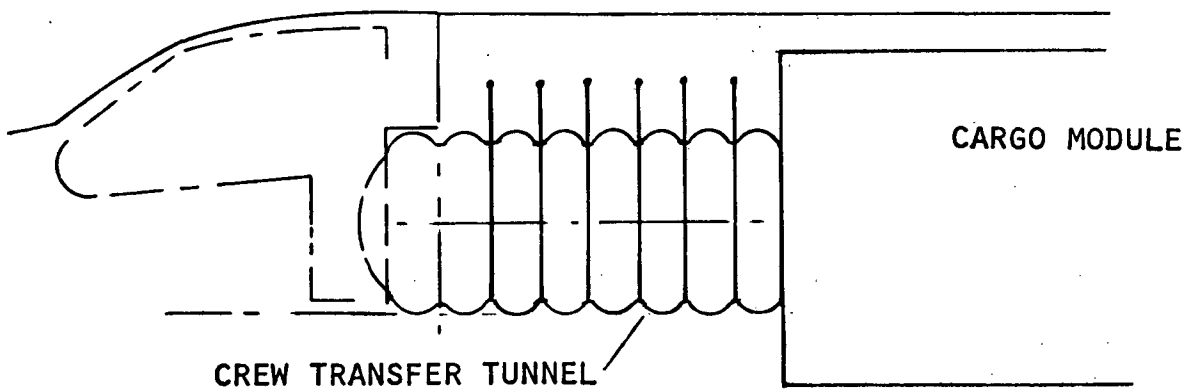


Figure 7. Configuration C Helical Spring

PACKAGED



DEPLOYED STRAIGHT



DEPLOYED CURVED

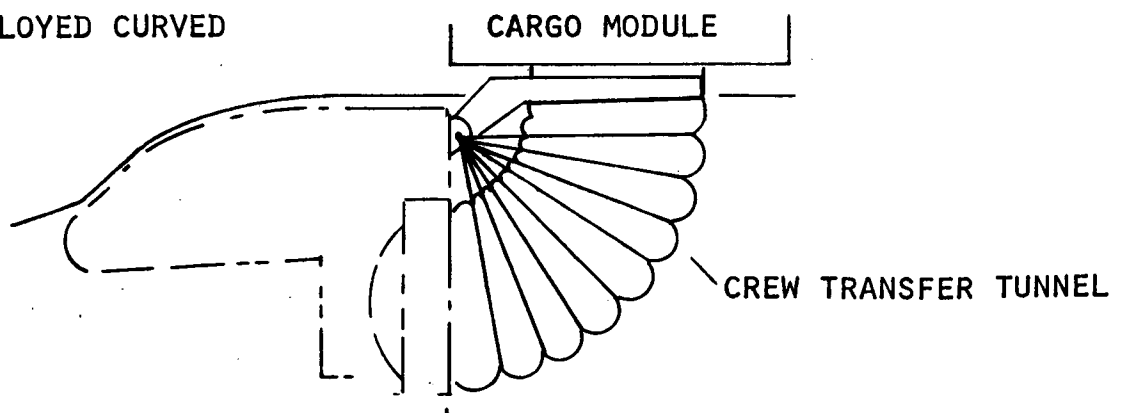
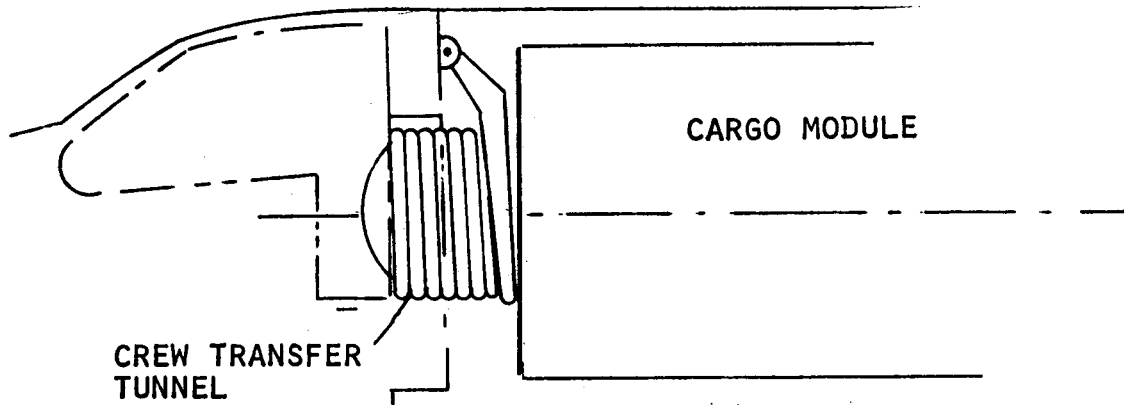
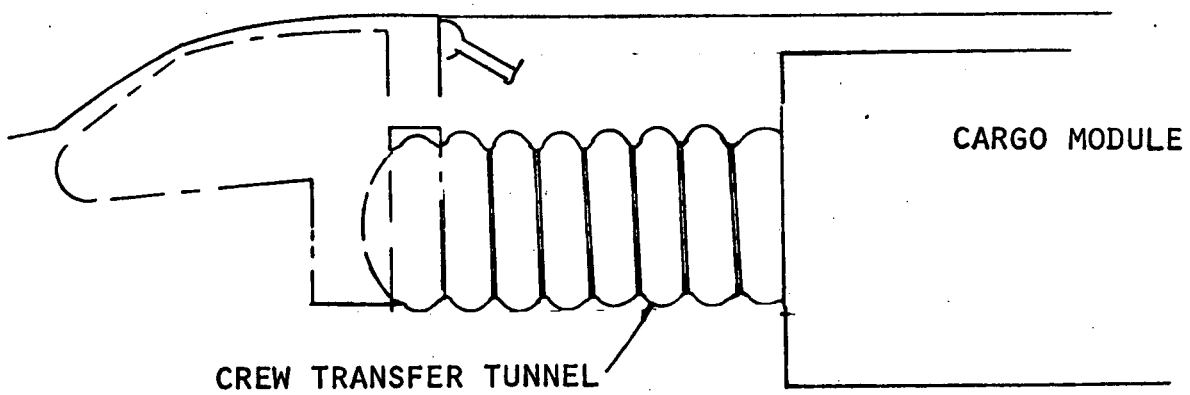


Figure 8. Configuration D Ring Supported Tunnel

PACKAGED



DEPLOYED STRAIGHT



DEPLOYED CURVED

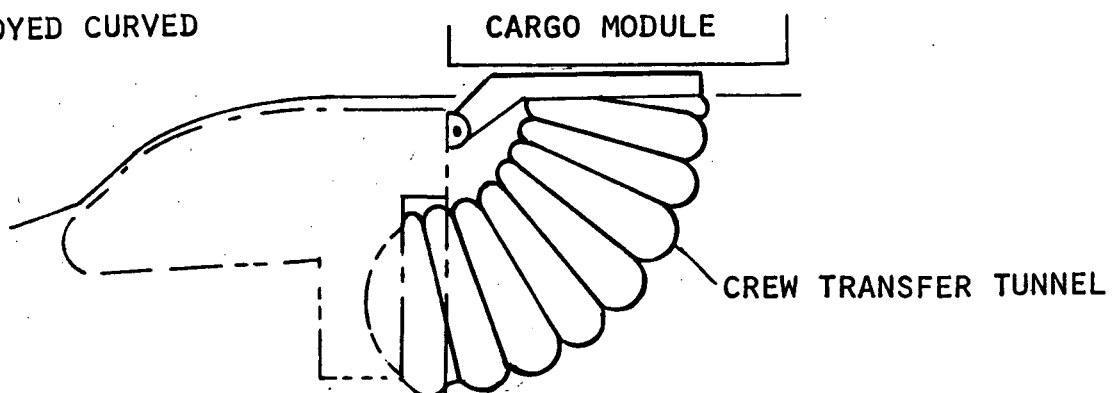


Figure 9. Configuration E Cable Supported Tunnel

### C. PRELIMINARY STUDY SUMMARY

The results of the preliminary study are presented in matrix format in Table I. The factors used in the comparison are listed in the left column and include configuration sizes, functional requirements, deployment mechanisms, fabrication techniques, and relative weights, reliabilities and costs. The study could be summarized as follows.

#### 1. Configurations A and B Truncated Cones and Spheres

These two configurations use proven techniques with state-of-the-art materials. Both types can be pressurized either packaged or fully deployed straight or curved. During deployment the tunnel cannot be fully pressurized. A ground change over function is required to re-configure the tunnel from a straight to curved type operation.

#### 2. Configuration C Helical Spring

In the preliminary analysis a realistic spring design did not appear feasible. It became evident during the analysis that the spring weight would be excessive and the package length too long.

#### 3. Configuration D Ring Supported Tunnel

The ring supported tunnel would meet all of the design and operational requirements including deployment curved or straight and pressurized or unpressurized. However, the deployment mechanism would be complicated and heavy.

#### 4. Configuration E Cable Supported Tunnel

The cable supported tunnel would meet all of the design and operational requirements including deployment curved or straight and pressurized or unpressurized. The proposed materials, except Fiber B, have been tested and qualified to similar requirements. Fiber B is presently being used on other military and NASA applications and would require only a nominal testing program to verify functional and environmental compatibility with tunnel requirements. Full-scale model testing should be accomplished to prove the concept.

### D. CABLE SUPPORTED TUNNEL MODEL

In order to more fully understand the operational characteristics of the cable supported tunnel a 1/4-scale model was fabricated and functionally tested. Figures 1, 2, and 3 show this model.

The model consisted of a urethane coated Nylon fabric cylinder attached to a fixed pressure tight bulkhead at one end and a movable pressure tight bulkhead at the other end. Six aluminum rings were positioned inside the cylinder at equal distances along the axis and attached to the fabric cylinder with external

Table I. Preliminary Study Results

	CONFIGURATION "A" TRUNCATED SPHERES	CONFIGURATION "B" TRUNCATED CONES	CONFIGURATION "C" HELICAL SPRING STR.	CONFIGURATION "D" RING SUPPORTED TUNNEL	CONFIGURATION "E" CABLE SUPPORTED TUNNEL
<b>FUNCTIONAL REQUIREMENTS</b>					
Deployed Straight Length	--	--	--	--	--
Packaged Length	53 Inches	Slightly Less Than 53 Inches	Package Length Greater than 80% of Deployed Length	≈ 0.5 of Config "A"	≈ same as Config. "A"
Deploy at Intermediate Straight Lengths	1. Not compatible with Filament Winding 2. Not stable in partially dep. position	Not stable in Partially deployed position	Yes	Yes	Yes-with some distortion
Deploy Curved	Yes	Yes	Yes	Yes	Yes-with some distortion
<b>Pressurization</b>	--	--	--	--	--
Deployed	Yes	Yes	Yes	Yes	Yes
During deployment	1. Unstable 2. High restrain- ing loads on dep. mechanism	No-same as Configuration "A"	Yes	Yes	Yes
During retraction	1. Unstable 2. High restraining loads on dep. mechanism	No-Same as Configuration "A"	Yes	Yes	Yes
Packaged	Yes-with restrain- ing cage	Yes-with restrain- ing cage	Yes	Yes	Yes
Ease of Operation	Requires a sequence of events, i.e. - air- lock closed - depressurization- deployment- repressurization- airlock opened	Essentially the same as Config. "A" (it will fold slightly easier)	Eliminates sequence	Eliminates sequence	Eliminates sequence
Tunnel Weights	400 pounds	Heavier than Config "A" ( ≈ 10 %)	Excessive	≈ 50% heavier than Config. "A"	≈ same as Config. "A"
<b>DEPLOYMENT MECHANISM</b>	--	--	--	--	--
Type	Similar to GD Proposed System	Similar to GD Proposed System	?	?	Cable, winch & hinge point
Shuttle Interface Req'ts	Similar to GD proposed system	Similar to GD proposed system	?	An order of magnitude greater moment req't than Config "A"	
Relative Weights	GD Deployment System 650 lbs	650 lbs	?	?	≈ Same as Config. "B"
<b>BETWEEN MISSION CHANGE- OVER REQUIREMENTS</b>	Curved to straight config. requires-removal, rotate segments and reinstallation	same as Config. "A"	None		
<b>TUNNEL FAB TECHNIQUE</b>	STR-Filament Wound Spherical Segments	STR-Patterned Fabric Cloth Layup	Fabric Cylinder & Spring	Fabric Cylinder & Titanium Rings	Fabric cylinder
<b>DEVELOPMENT STATUS</b>	State-of-the-art	State-of-the-art	Spring is of Questionable design	≈ 80% State-of-the- art	≈ 80% State-of- the-art
<b>LIFE LIMITING FACTORS</b>	1. Normal Operation greater than 100 cycles 2. Careless Human operation in 10 may be the most severe use	Improved Life expected with Fiber "B"	Similar to Config. "B"	Similar to Config. "B"	Similar to Config. "B"
<b>RELIABILITY</b>	High	High	High	Less than Config. "A" (more Components)	Less than Config. "A" (more Components)
<b>ENVIRONMENT COMPATIBILITY</b>	Good-with steel wire proven Good-with Fiber "B" Test Req'd	All material except Fiber "B" Proven-Expect Good results for Fiber "B"-Tests Required	Similar to Config. "B"	Similar to Config. "B"	Similar to Config. "B"
<b>RELATIVE TUNNEL COST DEV/UNIT</b>	\$850,000/ \$90,000	Lower than Config "A" due to reduced tooling ing/ Slightly Higher than Config. "A"	Higher than Config. "A" / Higher than Config "A"	Higher than Config. "A" / Higher than Config "A"	Higher than Config. "A" / Higher than Config. "A"
<b>ADVANTAGES</b>	1. Lightweight structure 2. Stable in fully deployed position either straight or curved 3. Similar structure has passed qualification tests 4. Same Tunnel can operate curved or straight	Essentially the same as Config. "A" except it has better folding characteristic; however, it weighs slightly more	Meets all Operational requirements but is heavy, expensive and has a long package length	Meets all Operational requirements and has a small package length	Meets all Operational Requirements
<b>DISADVANTAGES</b>	1. Unstable in partially deployed position with internal pressure 2. Cannot be pressurized during deploy- ment or retraction			Heavier than Config "A" and has a complex deployment Mechanism	Requires Development has poor esthetic qualities

clamp rings. The deployment force was obtained from the internal pressure and reacted by a series of cables, pulleys and weights. The cable, pulley and weight arrangement is shown in Figure 10. The cables pass through holes (fairleads) in each of the six rings thus controlling the transverse position of the rings. Longitudinal position of the ring was controlled by lobes of tunnel fabric. The direction of travel of the movable bulkhead is established by a hinge for curved deployment and guide rails for straight deployment.

Functional testing of this model confirmed the preliminary analysis predictions. The cable supported tunnel was therefore selected for preliminary design of a full-scale ground test model.

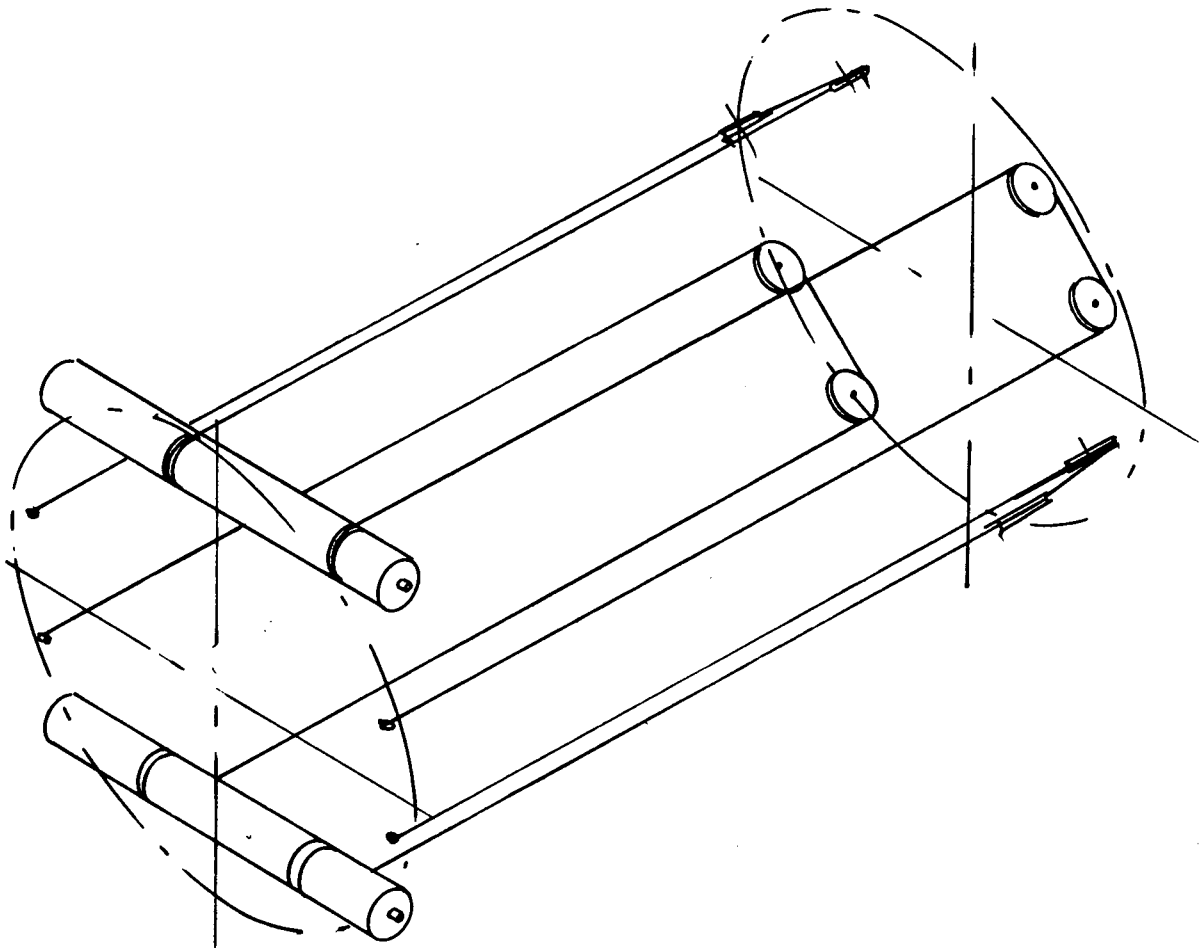


Figure 10. Cable Diagram

## SECTION IV

### SELECTED CONFIGURATION

#### A. GENERAL

Based on the preliminary study and favorable model tests, the cable-supported tunnel concept was selected for a more detailed study. The additional study included

- (1) preliminary design and analysis of a ground-test model
- (2) definition of the flexible structure materials, micrometeoroid properties, thermal properties, and
- (3) weight estimate.

In the interest of gaining the maximum amount of information for the least cost, the ground-test model design was based on

- (1) designing the flexible structure to meet the space shuttle requirements, and
- (2) design all other components such as bulkheads, rings, pulleys, pulley supports, and actuating mechanisms using readily available materials, processes and components.

A unit fabricated to this design would be suitable for functional, environmental, load, and life testing of the flexible structure.

#### B. FULL-SCALE MODEL

The full-scale ground-test model is defined in Drawings 72QS2228, Sheets 1 through 6. The envelope dimensions are shown schematically in Figure 11.

The tunnel is in essence an inflatable cylinder structure. Generally, inflatable cylinders are unstable at intermediate and radial positions; therefore, a system of cables and tension rings are incorporated to maintain tunnel stability at all deployment positions. End plates or bulkhead at the ends of the inflatable cylinder provide support points for the cable pulleys and serve as the attachment ring for the tunnel fabric. In addition, the end plates establishes the interface for the payload and space shuttle with the tunnel. The tunnel length, and therefore the payload position, is controlled by the length of the cables. Under constant pressure, the tunnel attempts to achieve maximum volume at all times. The restraining force is supplied by the cables, thus the paying in or out of the cables positions the payload and in turn controls the length of the tunnel.

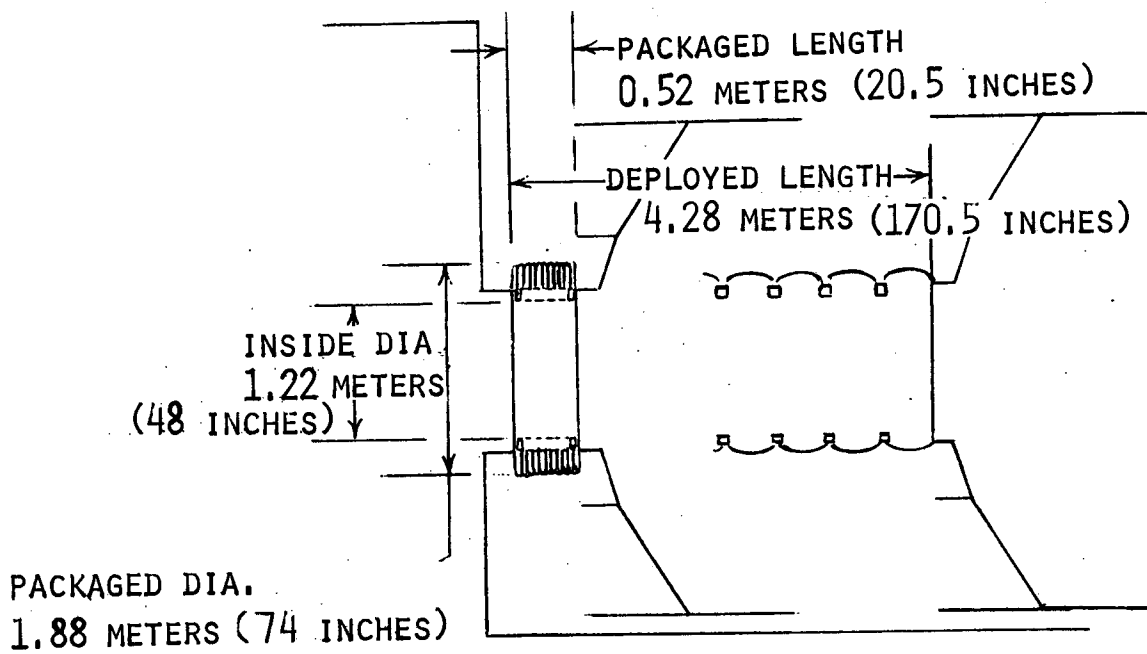
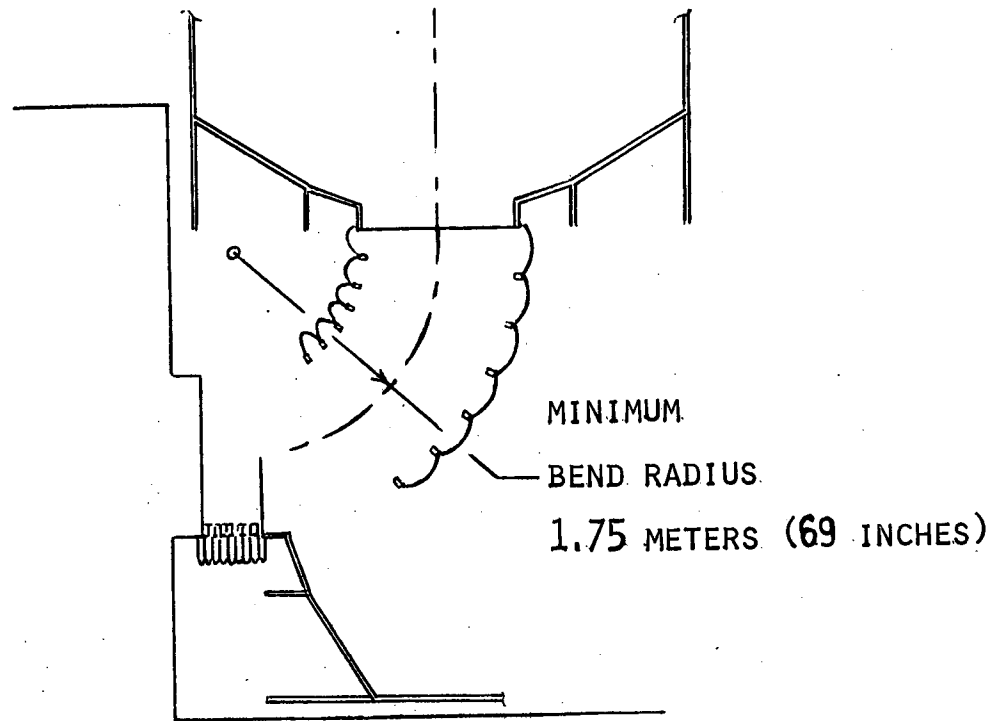


Figure 11. Envelope Dimensions

The winch or hoist controlling the length of the cables is envisioned as an electric motor driving a worm gear reduction transmission. Cable drums on the output shaft of the gear box take up or payout the cables. A screw thread shaft, also on the gear box output, maintains the position of a follower pulley for proper cable lead on the drum. For redundancy, the cables are rigged to provide a dual system, therefore maintaining a fail-safe tunnel in case of cable failure. Sheaves on the end bulkheads position the cables around the periphery of the tunnel, and the billowed bladder space the fairlead rings along the axis of the tunnel.

The tunnel wall or flexible structure is described in detail in Paragraph D of this section. It consists of four elements: inner pressure bladder, fabric structural sleeve, micrometeoroid barrier, and outer cover. The pressure bladder is made into a cylinder 1.88 meters (74 inches) in diameter and 4.98 meters (196 inches) in length. Dividing the cylinder into 40 equal sections circumferentially, the excess fabric is pleated to reduce the cylinder diameter to 1.37 meters (54 inches). At the fairlead ring locations, the pleats are bonded to establish a controlled fold geometry. The ends of the cylinder are configured to a 1.46 meter (57.5 inch) diameter sleeve and adapted to the seal rings. Additional ply strips are bonded between the pleat folds to attain a smooth surface at the ring clamps and seal face.

The fabric sleeve is made of Fiber B material. Major loads on the fabric are axial; therefore, the fabric splice seams run the length of the cylinder. A return seam or hem on the ends of the cylinder with a metal plate insert prevents fabric slippage under the seal ring. Construction and dimensions of the fabric sleeve are similar to those of the bladder. Pleat folds and the added strip for uniform thickness at the clamps, however, are sewed in position. To form a composite structure, the bladder is inserted within the sleeve; The pleats are matched and the units bonded together in the clamp areas.

Construction of the micrometeoroid barrier and outer cover follow the procedure used on the bladder. A 1.27 cm (0.5 inch) thickness of foam bonded to a bias-close woven fabric forms the cross section for the tunnel cover. After the cylinder is pleated, a fabric tape sewed over the foam in the clamp areas retain the folds. The blanket is configured to be incorporated after the bladder and Fiber B sleeve are installed on the tunnel rings.

Eight rings are incorporated in the tunnel design. These rings serve as support for the cable guides, provide structure for variable fabric loading, stabilize the clamps under pretension loads, and act as step or ladder rungs during tunnel egress and ingress. The rings are a weldment made of two-inch square steel tubes rolled to a 1.37 meters (54 inches) diameter. Round tubes to contain the cable fairlead are incorporated in the rings. Associated with the rings are steel bands which are made up into three-section clamps for serving the inflatable structure to the rings. Provisions are also made on these bands to position hose-type clamps for the thermal and meteoroid cover installation.

The end plates or bulkheads are aluminum weldments made from 6061 sheet and plate stock. The flight article would be similar in geometry and function; however, an appreciable weight savings could be made possible by incorporating more refined methods of analyses and higher strength materials. The end plates have a cross section approximating a "C" section. A flange welded to the out-board leg of the channel establishes an interface for the tunnel with payload and crew compartment. It also becomes the attachment flange for the tunnel fabric. O-ring grooves on the flange provided the pressure seals at the tunnel interface. The inboard flange, incorporated on the end plates, resist the torsional forces applied to the section. The aft face of the section serves as the attachment structure for the floating pulleys and cables.

The cable system controlling the tunnel position consists of four stainless steel wire ropes 1.11 cm (0.437 inch) diameter. Each wire rope traverses the length of the tunnel, reversing the direction over pulleys on the end plate, resulting in a total of 12 cables equally spaced around the periphery of the tunnel ring. The cable pattern is such that failure of one cable still retains a safe condition. In addition, all cables travel the same distance, even during the transition phase when the payload is rotated 90°.

Cable sheaves have a cable-to-sheave diameter ratio of 16. The pulleys are made from 2024 aluminum and because of cable loads, a double row of aircraft ball bearings with 1.59 cm (0.625 inch) bore is incorporated. The pulleys are supported from hangers which are steel weldment, configured such that the resultant cable loads pass through the axis of hanger rotation. Since the cables have an angular change during payload rotation, pulley hangers have a self-alignment capability of 30°. Guards are also incorporated to retain cables on the pulleys in case slack occurs in the system.

To further understand the tunnel concept, the procedure for assembling the tunnel structure is depicted. Fairleads are temporarily installed on the fairlead rings and the rings are stacked so that all fairleads align. The tunnel fabric structure is worked over the rings and positioned axially on the rings where the pleats are bonded. Steel clamps are incorporated over the rings and pretensioned to the extent that compression still exists on the ring when the tunnel is pressurized.

Pulleys and their hangers are installed on the end plates. Cables are then strung through the sheaves and ring fairleads (incorporated at this time), terminating at swaged fittings on the payload bulkhead. The bitter ends of the cable are secured to the winch drum at a later time.

With cables in proper alignment, O-rings are placed in grooves on the end plates and the meteoroid-thermal blanket is slid over the tunnel. The tunnel fabric, held by the seal ring, is bolted to the end plate interface. After checkout for leakage in the structure, the tunnel cover or meteoroid shield is positioned and secured with hose clamps to the fairlead rings and seal rings. To achieve the packaged shape, pressure is applied to the tunnel for shaping the fabric walls.

## C. STRUCTURAL ANALYSIS

### 1. General

The purpose of this analysis was to substantiate the feasibility of the design and to determine the strength requirements of the structure with sufficient accuracy so that a weight estimate could be made.

The environmental and load requirements of the space shuttle tunnel is given in Section II of this report. These requirements include the initial requirements and also up-dated requirements established during the program.

A structural analysis covering the principal structural members (rings, fabric and cables) is presented in Appendix I. For those structural components, such as fittings, pulleys and brackets which were not analyzed, a reasonably accurate estimate of the weight was made without a detailed stress analysis.

### 2. Analysis Summary

The work statement requires that:

- (a) The tunnel be able to withstand an internal pressure after deployment of 102.730 newtons/sq meter (14.9 psi)
- (b) The tunnel be capable of withstanding the environment given in Section II and be capable of functioning after exposure to the environment.
- (c) A factor of safety of three be maintained throughout the structure.
- (d) The tunnel shall function at any altitude from sea level to 833,400 meters (450 nautical miles).
- (e) The minimum inside diameter of the tunnel shall be 1.22 meters (48 inches).
- (f) The number of allowable deployment cycles be determined.
- (g) The approximate forces required for unpressurized deployment and retraction be determined.

The design as shown by the Appendix I analysis meets items (a) through (e) above. The allowable deployment cycles (item f) has been established as 200. The approximate forces required for unpressurized deployment and retraction have been determined as 1500 newtons (350 pounds)(see Appendix I).

## D. MATERIAL SELECTION (EXPANDABLE STRUCTURE)

### 1. General

The materials approach selected in the design of the expandable structure portion of the flexible tunnel is based on a four-layer composite material. This composite consists of an unstressed inner layer functioning as a pressure bladder for gas retention, a structural layer which carries the transmitted pressure loads, a micrometeoroid barrier which prevents penetration of the pressure bladder by high-velocity particles, and an outer cover which encapsulates the total material composite and provides a smooth surface for the application of a thermal control coating.

The materials selection is based on existing technology (Figure 12) for expandable structure materials as represented by the combined technologies of the Air Force D-21 Expandable Airlock Experiment (Contract F33615-67-C-1380), the NASA-LRC Lunar Shelter (Contract NAS1-4277), and Moby Dick Expandable Structures Module (Contract NAS1-6673), developed by Goodyear Aerospace Corporation. Figure 13 depicts this development, showing a diagram of the four-layer composite material concept.

The four-layer composite structure is described as follows:

### 2. Outer Cover Layer

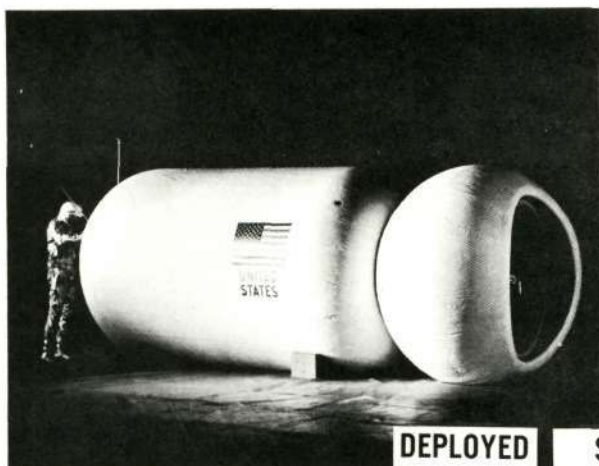
The outer cover consists of a Film-Fabric laminate of Capran (nylon) film and 23.7 gm/sq meter (1.0 oz/sq yd) nylon fabric as illustrated in Figure 14. The outer fabric layer provides a smooth base for the application of a thermal control coating. A silicone-type coating is painted on the outer cover surface with the proper pigmentation as determined by the supporting thermal analysis for thermal control.

### 3. Structural Layer

A layup construction utilizing DuPont Fiber B woven cloth is utilized for the structural layer and provides near the optimum in lightweight load carrying flexible structure. The selected cloth weight is 296 gm/sq meter (12.5 oz/sq yd) and is shown in Table II under Cloth "B" specification.

### 4. Micrometeoroid Layer

To provide the penetration resistance as determined by the micrometeoroid hazard assessment, 1.27 cm (1/2-inch) thick flexible polyether open cell foam of 15.4 gm/cu meter (1.2 pcf) density was selected. The foam is encapsulated by the outer cover layer and by a 23.7 gm/sq meter (1.0 oz/sq yd) cloth layer adjacent to the structural layer. Time-load tests conducted on small samples

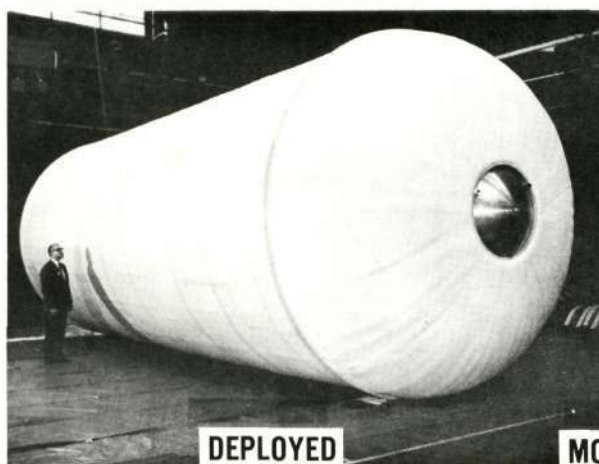


DEPLOYED

STEM

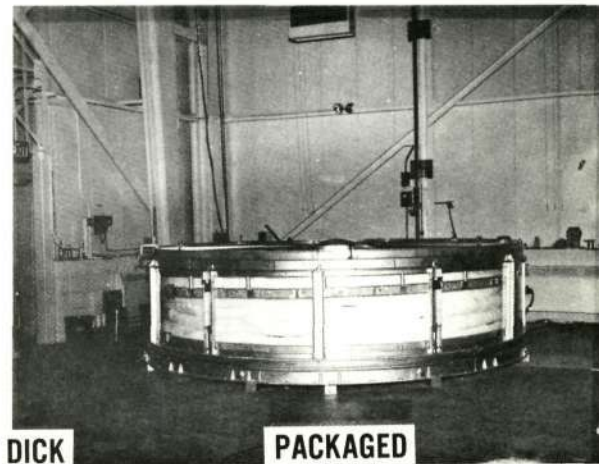


PACKAGED



DEPLOYED

MOBY DICK

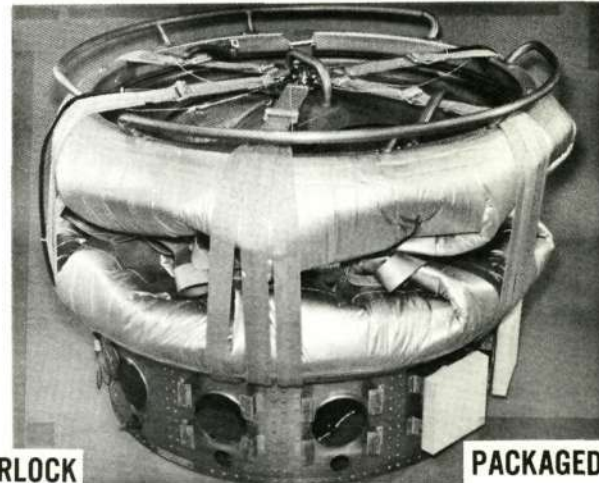


PACKAGED



DEPLOYED

D-21 AIRLOCK



PACKAGED

Figure 12. Existing Technology

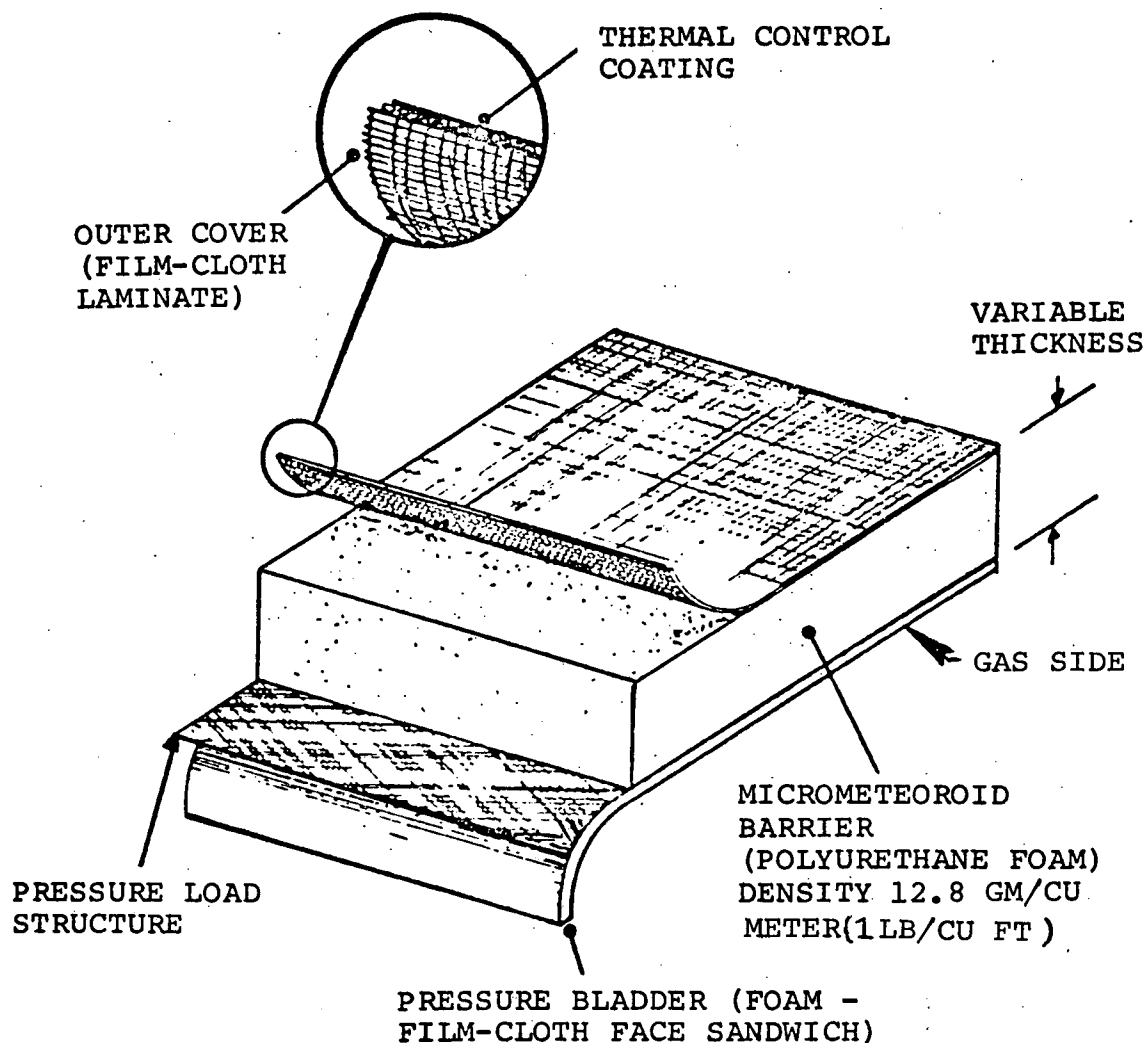


Figure 13. Elastic Recovery Materials Technique

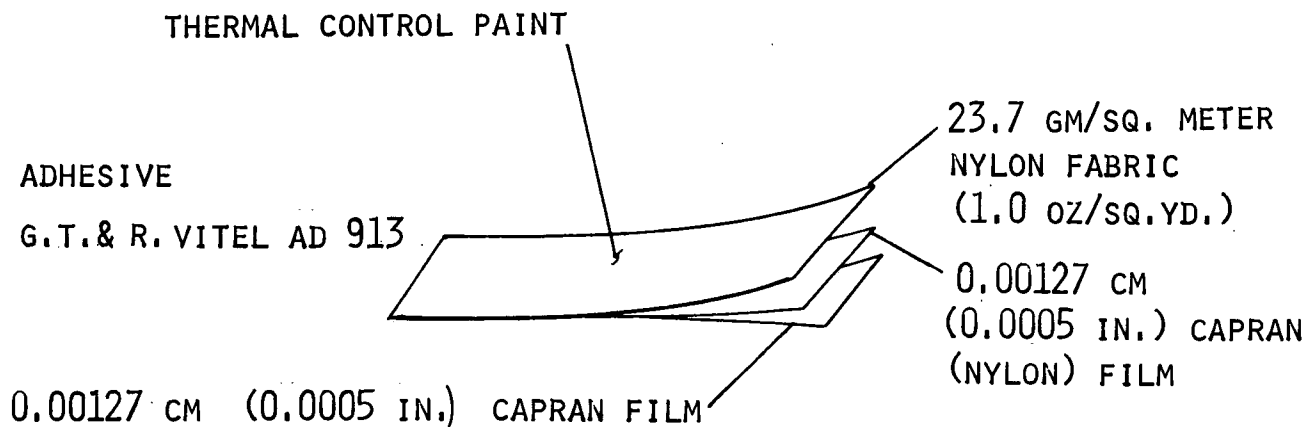


Figure 14. Outer Cover

TABLE II  
FIBER B WOVEN CLOTH SPECIFICATION  
SUMMARY

	Cloth A	Cloth B	Cloth C	Cloth D	Cloth E	Cloth RF-138
Weave	Basket	Plain	Basket	Basket	Basket	Basket
	1/3	1/1	1/2	1/2	4/6	2 x 2
Count						
Warp	20	15	15	15	32	28
Fill	32	15	25	20	53	28
(Ends/Inch)						
Strength						
Warp	2000	1500	1500	1500	3200	1200
Fill	3200	1500	2500	2000	5300	1200
(#/Inch)						
Weight	21.5	12.5	16.5	14.5	33.5	12.0
(OZ/YD <sup>2</sup> )						
Thickness	.050	.025	.035	.030	.060	
(Inches)						
Width	60	60	60	60	60	20
(Inches)						
Yarn	1500/1/2	1500/1/2	1500/1/2	1500/1/2	1500/1/2	1500/1
Construction	3TP1	3TP1	3TP1	3TP1	3TP1	0.5TP1
Yarn Code	EYDB-40	EYDB-40	EYDB-4	EYDB-40	EYDB-40	EYDB-40
Yarn Type	DP-01	DP-01	DP-01	DP-01	DP-01	DP-01

of the foam were used to ascertain the maximum length of time the composite structure can be packaged with a high reliability of elastic recovery when unpackaged. Figure 15 shows the recovery characteristics of the foam under vacuum conditions and for varying temperatures. From Figure 15 it can be seen that the packaged structure must be insulated against extreme cold if full recovery is to be achieved. In case the composite structure could not be insulated, a laminated micrometeoroid barrier construction consisting of a quilted blanket of 12.8 gms/cu meter (1.0 pcf) curly woven (Owens Corning heat-set glass filaments) would provide 195°K (-100°F) flexibility. The resilience of the curly wool permits it to be compressed for packaging with an expansion following deployment of the structure. The filaments have no chemical lubricant and will not burn.

## 5. Pressure Bladder

The pressure bladder is a composite of several layers as shown on Figure 16. A triple gas barrier is provided by the two film-fabric laminates and the closed cell EPT foam. This three-layer composite provides a cushioning effect to achieve greater puncture resistance against sharp object contact. Any single layer can be pierced without making a leak path. The inner foil layer is multifunctional. The primary purpose is to act as a flame barrier against flash ignition sources, but it also provides improved scuff resistance to the bladder and in combination with the alodine coating, provides passive thermal control.

## 6. Composite Fabric Weight

The unit weight breakdown of each component is shown in Table III.

Table III. Unit Weight Breakdown

<u>Construction Component</u>	<u>gms/meter<sup>2</sup></u>	<u>Weight - PSF</u>
Aluminum Inner Layer	0.168	0.004
Adhesive	0.421	0.010
Pressure Bladder	4.460	0.106
Adhesive	0.420	0.010
Structural Layer	3.663	0.087
Inner Cover	0.295	0.007
Polyurethane Foam	3.536	0.084
Adhesive	0.421	0.010
Outer Cover and Coating	<u>2.610</u>	<u>0.062</u>
Total	15.995	0.380

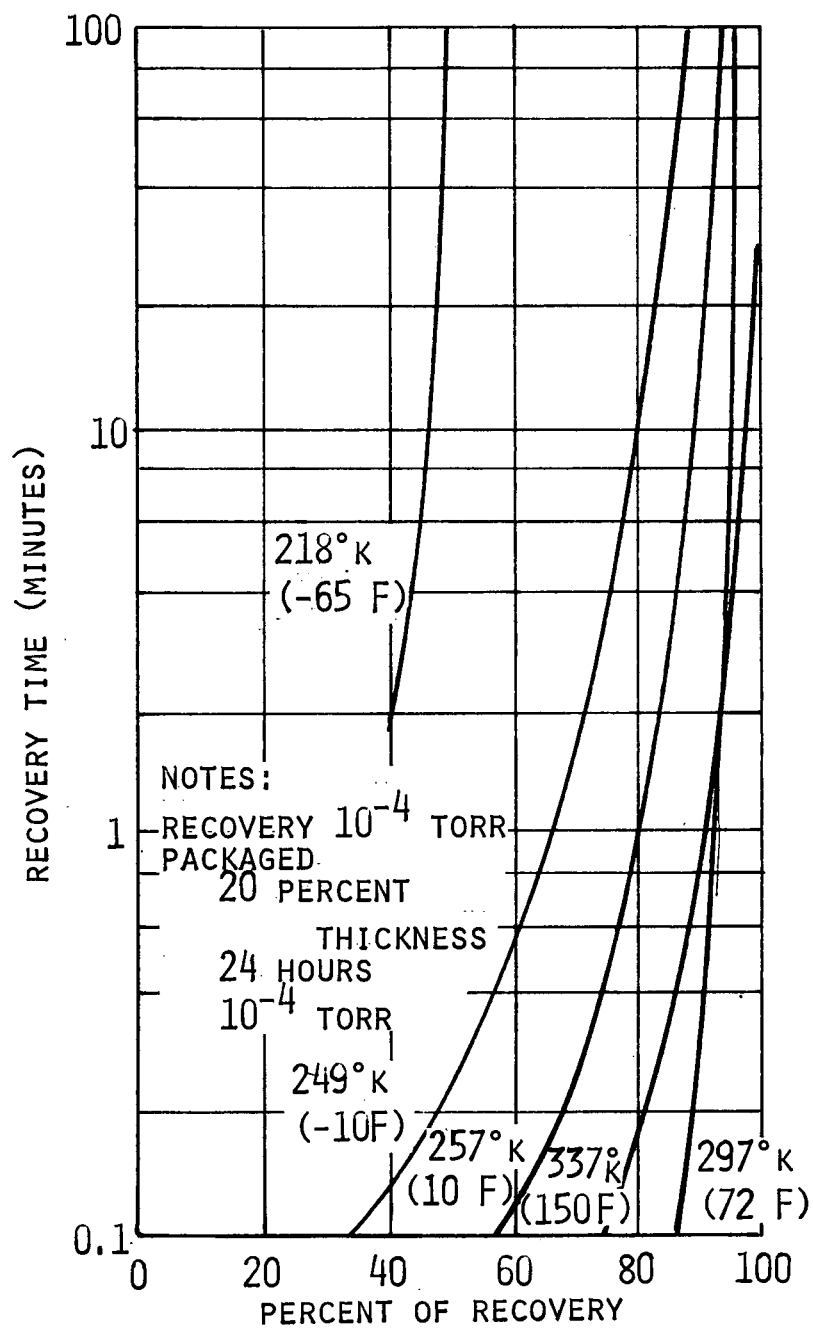
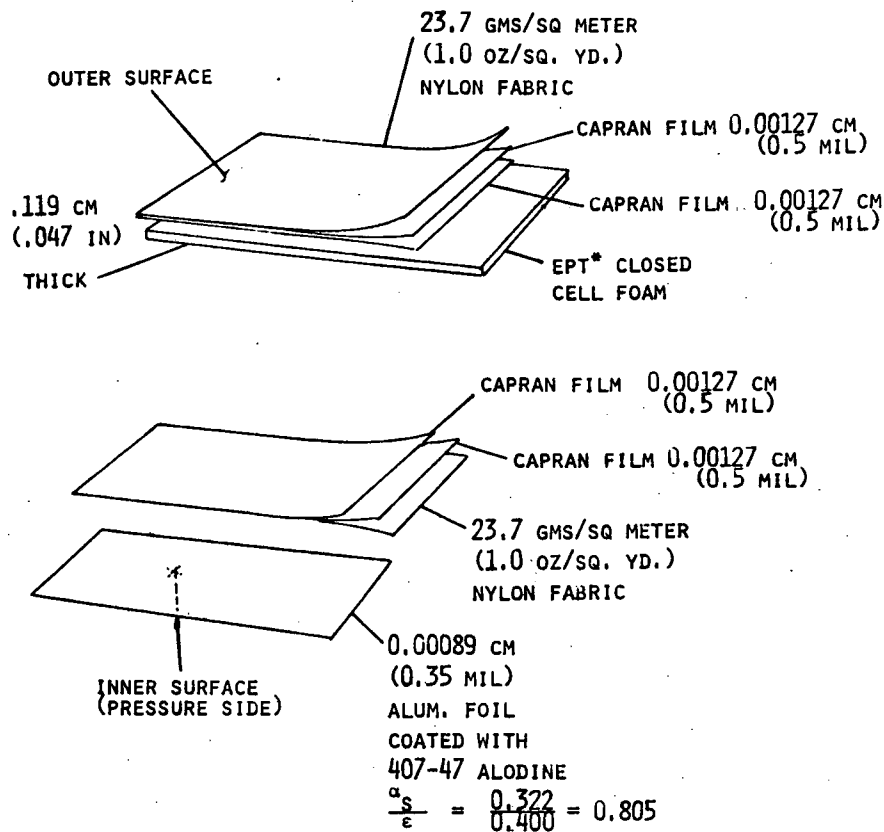


Figure 15. Foam Thickness Recovery Versus Time



\* - ETHYLENE PROPYLENE TERPOLYMER (RUBATEX R-481-T)

Figure 16. Pressure Bladder

## 7. Environmental Compatibility

The compatibility of the expandable materials with respect to operations in a space environment has been established with extensive ground testing. Table IV presents the environmental compatibility characteristics of the selected materials. The materials capability indicated is well within the range of expected environmental conditions without constraining the basic shuttle flight in any way.

Substantiating data for use of the D-21 Airlock nonmetallic materials in accordance with acceptance guidelines and test requirements for nonmetallic materials in the Apollo spacecraft are given in Reference 1.

### E. MICROMETEOROID ANALYSIS

#### 1. General

The deployment of the Flexible Tunnel during orbital flight of the Space Shuttle Vehicle will expose this tunnel to a meteoroid environment. Exposure

Table IV. Environmental Compatibility - Expandable  
Materials

Toxicity: Non-detectable

Flame Resistance: 0.00089 cm (0.3 mil) Alum Foil Flame Barrier  
(Self-Extinguishing)

#### Thermal Characteristics

Max. Temperature (Short Term Exposure - No Stress)

Outer Surface Materials	420°K (+300°F)
Inner Surface Materials	394°K (+250°F)

Max. Temperature (Long Term)	346°K (+165°F)
------------------------------	----------------

Min. Temperature  
(Using Quilted Blanket Micrometeoroid Barrier)

Deployment Flexibility	199°K (-100°F)
Expanded Static	172°K (-150°F)

(Using Polyurethane Foam Micrometeoroid Barrier)

Deployment Flexibility	242°K (-25°F)
Expanded Static	172°K (-150°F)

#### Vacuum Effects

1/2% Weight Loss at  $10^{-6}$  TPRR

#### Space Radiation

Material Tolerance	$10^7$ Rad
Expected Dose (1-Year)	$10^5$ Rad

to this environment yields a possibility of a meteoroid penetration and a subsequent loss of pressure in the flexible tunnel. In conjunction with the tunnel study, a preliminary analysis was conducted to determine the thickness of micrometeoroid bumper material that would be required to absorb the meteoroid impacts. This section of the report summarizes the considerations given to the meteoroid environment and the results obtained from the analysis.

The flexible tunnel at the shuttle craft/payload interface is to function in near-earth orbit at altitudes out to 450 nautical miles. At the present time, a seven-day mission time has been envisioned as typical for tunnel exposure time during orbital flight. The flexible tunnel must be capable of being used in either of two positions as shown schematically in Figure 17. In the extended

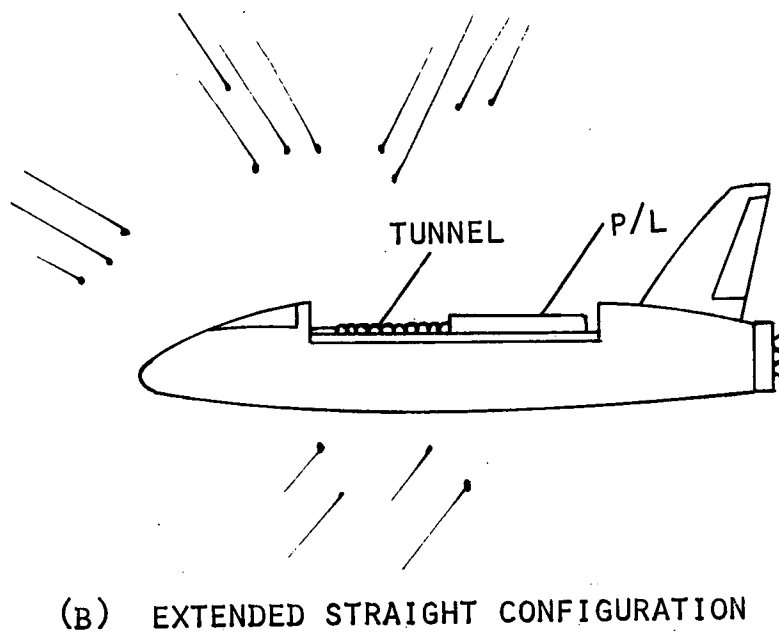
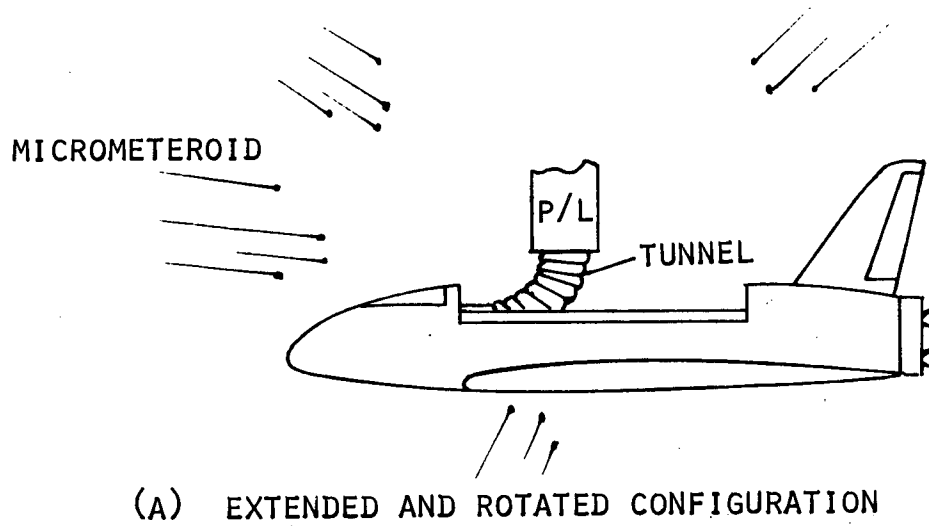


Figure 17. Schematic of Micrometeoroid Hazard to Tunnel

straight configuration, the tunnel will be contained in the shuttle payload section and to a large degree will be protected from the micrometeoroid environment by the shuttle craft structure. In the extended and rotated configuration, the tunnel will be exposed to a greater extent to micrometeoroid hazard. However, the shuttle craft as well as the payload will still shield the tunnel to some degree.

## 2. Micrometeoroid Environment

The average cumulate meteoroid distribution for preliminary design purposes has been specified in Reference 2 to be given by the following equation

$$\log_{10} N_t = -14.37 - 1.213 \log_{10} m \quad (1)$$

for a particle mass range of

$$10^{-6} \leq m \leq 10^0$$

where  $N_t$  = number of particles of mass (m) or greater per square meter per second

$m$  = particle mass, grams

This mass density of the meteoroid particles in this distribution is specified to be  $0.5 \text{ gm/cm}^3$  while the average meteoroid velocity is specified to be 20 km/sec.

The actual flux density of meteoroid particles can be obtained by the following expression

$$N = N_t G_e \zeta \quad (2)$$

where  $N_z$  = gravitationally focused unshielded flux, equation (1)

$G_e$  = defocusing factor for earth

$\zeta$  = body shielding factor

This expression corrects the unshielded and gravitationally focused flux for the defocusing effect of the earth and the shielding of the component or tunnel in this case by other parts of the spacecraft. The defocusing factor

( $G_e$ ) is presented graphically in Reference 3 while the shielding factor ( $\zeta$ ) must be determined uniquely on a geometric relationship basis to the spacecraft.

### 3. Probability of Impact

The number of particles (I) of mass (m) or greater which may impact the tunnel can now be written as

$$I = NA\tau \quad (3)$$

where

I = number of particles of mass (m) or greater impacting the tunnel

N = corrected flux density of meteoroid particles, particles, per square meter per second

A = impact area, square meters

$\tau$  = exposure time, seconds

Assuming a Poisson distribution, it is then possible to write an expression for the probability ( $P_k$ ) for any number (k) of particles of mass (m) or greater to impact the tunnel. This can be written as

$$P_k = I^k e^{-I}/k! \quad (4)$$

The probability of no penetrations ( $P_0$ ) of the tunnel due to meteoroid impact is then

$$P_0 = e^{-I} = e^{-NA\tau} \quad (5)$$

By combining equations (1), (2), and (5), the design meteoroid mass can be obtained. The resulting equation is

$$m_m = \left\{ - \frac{G_e \zeta A}{10^{14.37} (\ln P_0)} \right\}^{\frac{1}{1.213}} \quad (6)$$

The resulting mass (m), combined with the average velocity and average density of the meteoroid particle gives the meteoroid energy which must be absorbed by the bumper.

#### 4. Meteoroid Mass Calculation

The maximum mass of the impacting meteoroid may now be calculated for a specified value of probability of no penetration of the meteoroid bumper shield. The following orbital conditions have been specified earlier:

$$\text{Altitude} \leq 833 \text{ km (450 N.M.)}$$

$$\text{Mission time} \leq 7 \text{ days} = 6.05 \times 10^5 \text{ seconds}$$

The defocusing factor of the earth at an altitude of 833 km (450 nautical miles) is

$$G_e = 0.94$$

This factor approaches unity as the altitude decreases. The vehicle shielding factor is assumed to be

$$\zeta = 0.80$$

for the extended and rotated position of the tunnel. This allows for some shielding effect from the payload and the shuttle vehicle. In the extended straight position, the shielded factor will be somewhat less than for the extended/rotated position of the tunnel.

The surface area is assumed to be

$$A = 23.25 \text{ square meters (250 ft}^2\text{)}$$

Thus, for a tunnel diameter of 1.22 meters (4 feet), the length of the tunnel would be approximately 6 meters (20 feet).

Equation (6) may now be evaluated if a probability of a no penetration ( $P_o$ ) is assumed. Thus, the design meteoroid mass is

$$m_m = \left\{ - \frac{(0.94) (0.80) (23.25) (6.05) \times 10^5}{10^{14.37} (\ln P_o)} \right\}^{0.824}$$

Evaluating this expression for

$$P = 0.995$$

the resulting meteoroid mass is

$$m_m = 0.105 \text{ mg}$$

while for a probability of no penetrations value of

$$P_o = 0.999$$

the resulting meteoroid mass is

$$m_m = 0.295 \text{ mg}$$

#### 5. Micrometeoroid Shield Thickness

The micrometeoroid shield thickness was calculated on the basis of the largest meteoroid particle that must be arrested during orbital flight and penetration test data obtained during a previous program at Goodyear Aerospace Corporation. The calculations of the limiting particle mass sizes have been presented while penetration test data for a polyurethane foam micrometeoroid shield is presented in Figure 18. This test data was taken directly from Reference 4. The test data was obtained by firing glass pellets at the foam targets from a light-gas gun at projectile velocities of about six km/sec. The outer surface of the foam was covered by two layers of No. 182 fiberglass cloth impregnated with a polyurethane elastomer, while the back side was formed by an aluminum witness plate. The density of the projectiles used during the test program was approximately  $2.8 \text{ gm/cm}^3$ . The foam thickness for the tunnel micrometeoroid shield was estimated by entering Figure 18 with a projectile mass computed using the following relationship taken from Reference 5:

$$m_m = (\rho_p / \rho_m)^{0.421} (V_p / V_m)^{1.895} m_p \quad (7)$$

where

$$m_m = \text{design meteoroid mass, mg}$$

$$m_p = \text{projectile mass, mg}$$

$$V_p = \text{projectile velocity, km/sec}$$

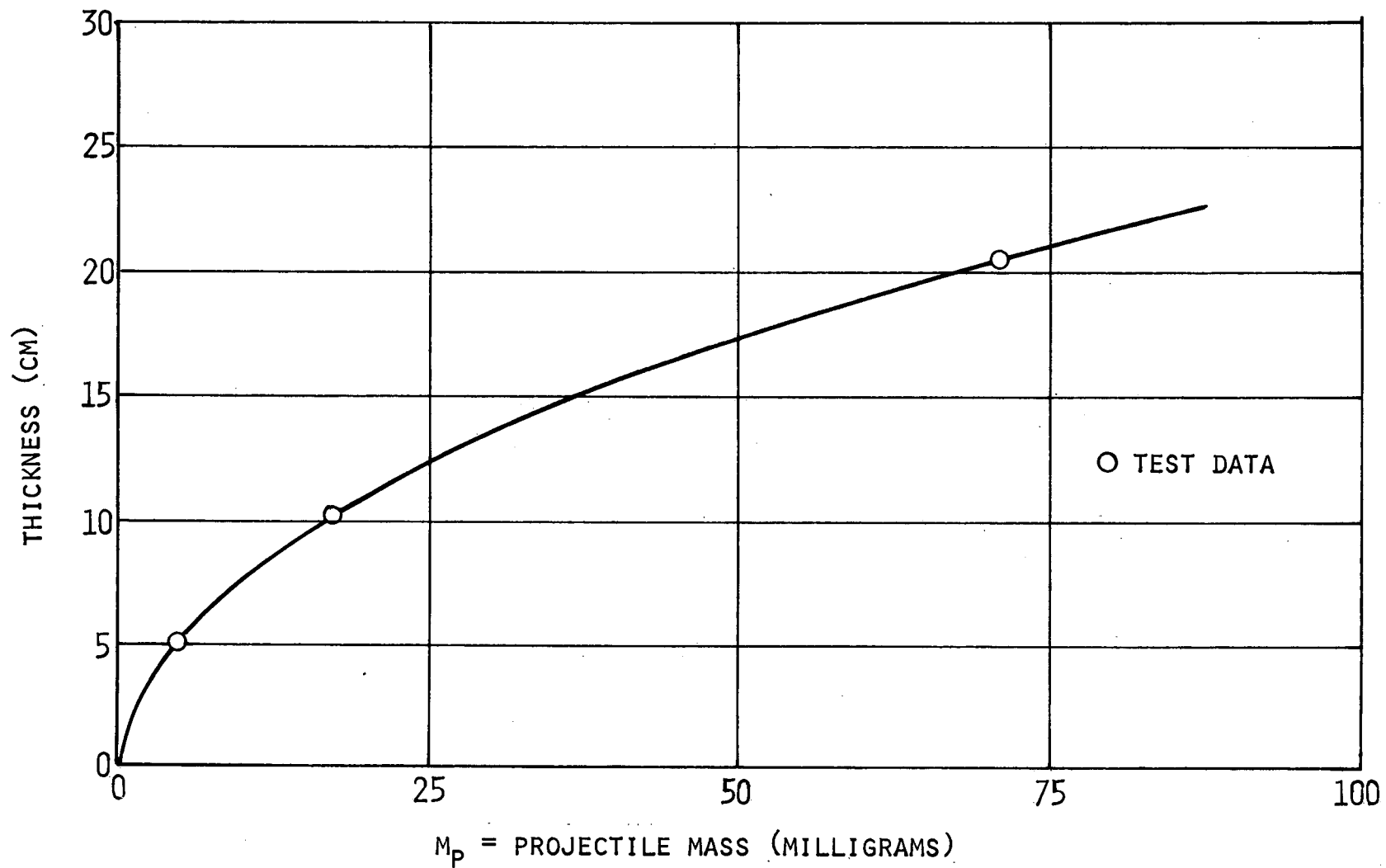


Figure 18. Foam Thickness vs Projectile Weight  
 $V_p \sim 6 \text{ KM/SEC}$

$V_m$  = meteoroid velocity, km/sec

$\rho_m$  = density of meteoroid, gm/cm<sup>3</sup>

$\rho_p$  = density of projectile, gm/cm<sup>3</sup>

Thus for a probability ( $P_o$ ) of 0.995 of no penetration of the wall by meteoroids larger than

$$m_m = 0.105 \text{ mg}$$

the equivalent projectile mass would be

$$m_p = 0.675 \text{ mg}$$

For a probability ( $P_o$ ) of 0.999 of no penetrations of wall by meteoroids larger than

$$m_m = 0.295 \text{ mg}$$

the equivalent projectile mass would be

$$m_p = 1.9 \text{ mg}$$

Entering Figure 18 with these projectile-mass values yields the following micrometeoroid shield thicknesses:

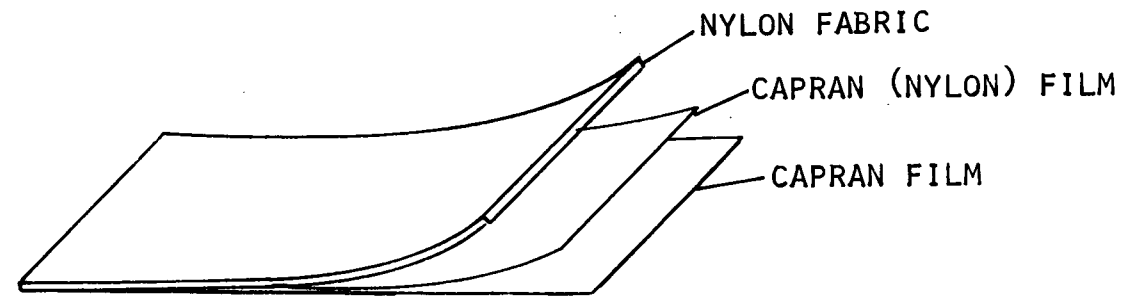
$$t \cong 1.0 \text{ cm (0.3937 inch) for } P_o = 0.995$$

$$t \cong 2.54 \text{ cm (1.0 inch) for } P_o = 0.999$$

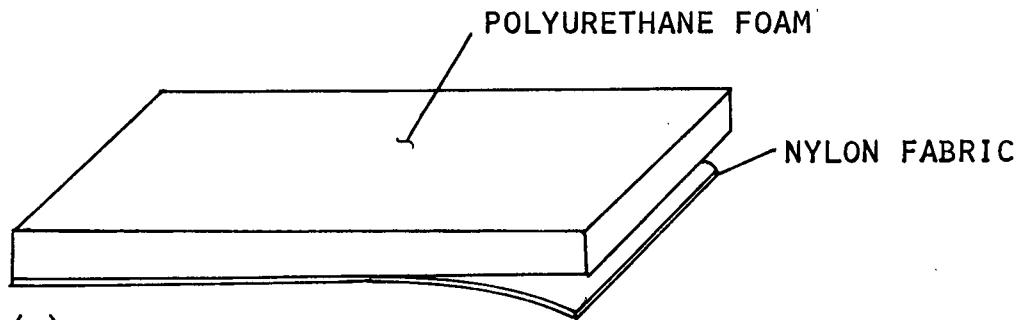
## F. THERMAL PROPERTIES OF TUNNEL WALL

### 1. Tunnel Wall Configuration

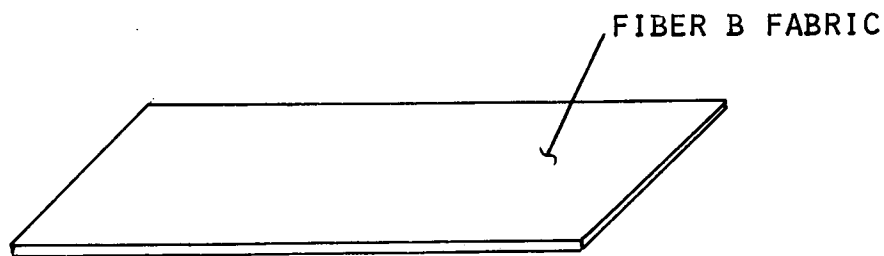
A schematic of the tunnel wall materials is presented in Figure 19. For purposes of this illustration, the wall construction has been broken down into four components. These are



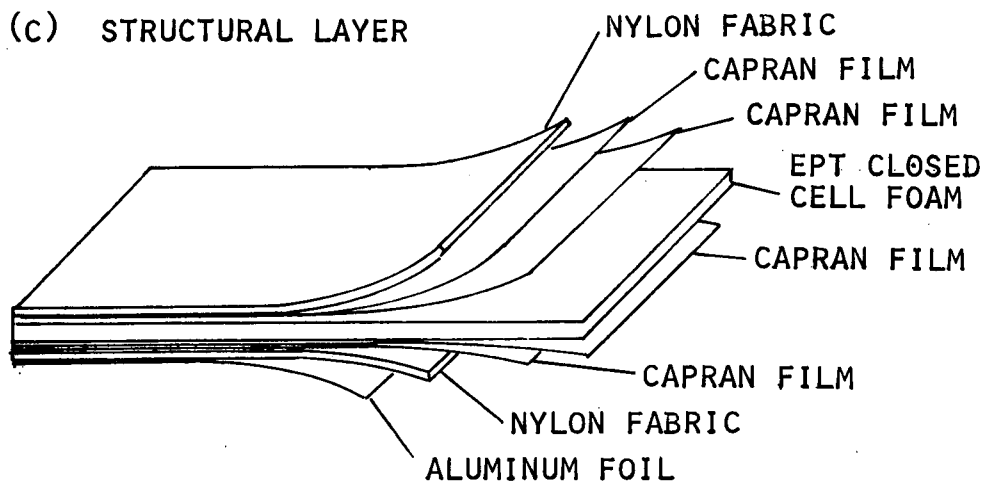
(A) OUTER COVER



(B) MICROMETEOROID SHIELD



(C) STRUCTURAL LAYER



(D) PRESSURE BLADDER

Figure 19. Schematic of Tunnel Wall Materials

- (a) the outer cover
- (b) the micrometeoroid shield
- (c) the structural layer
- (d) the pressure bladder.

The outer cover consists of a nylon fabric material on to which is bonded two layers of capran film. The outer surface of the nylon may be coated or painted to obtained desirable thermal radiation properties. The second component will consist of the micrometeoroid shield which is bonded to a nylon fabric. The third component is the structural layer which will be a Fiber B fabric. The innermost component will be the pressure bladder. This pressure bladder will be a composite consisting of a nylon fabric, two layers of capran film, ethylene propylene terpolymer (ETP) closed cell foam, two layers of capran film, and a layer of nylon fabric. The inside surface of the tunnel wall will be formed by a layer of aluminum foil.

## 2. Thermal Properties of Tunnel Wall Material

The thermal properties of the tunnel wall materials are presented in Table V in the same order as they were presented in the schematic diagram of the wall configuration shown in Figure 19. The density of the fabric material is not presented in Table V since it is more common to present this data in weight per unit area.

## G. WEIGHT ESTIMATE

The weight estimate for the flexible tunnel is shown in Table VI. The estimate is for all components including end attachment fittings but does not include the interface bulkhead or the cable drive mechanism. It is assumed that the interface bulkheads will be a part of the shuttle craft and payload vehicle. Sufficient design effort has not been completed to accurately estimate the weight of the drive mechanism.

The tunnel weights shown in Table VI were calculated for ground test model and estimated for the flight test model. The ground test is heavier than the flight test unit because the metal parts such as rings, clamp rings and pulley brackets were designed utilizing the most economical materials and fabrication methods. All flexible components of both tunnels are identical. With this philosophy, the maximum amount of data can be obtained on the ground test model at minimum cost.

The tunnel weight is heavier than previously predicted; however, consideration must be given to the fact that the tunnel deployment method either eliminates or severely reduces the sortie lab deployment requirements. This reduction in deployment load requirements should result in a weight savings in the Sortie lab deployment mechanism that more than compensates for the increase in tunnel weight.

Table V. Thermal Properties of Wall Materials

Component	Material	Density (gm/cm <sup>3</sup> )	Specific Heat (cal/gm-°C)	Thermal Conductivity (cal/gm-cm <sup>2</sup> -°C/cm)	Thickness (cm)
Outer Cover	Nylon	(34 gm/m <sup>2</sup> )	0.4	$3.31 \times 10^{-5}$	
	Capran				0.00127
	Capran				0.00127
Shield	Polyurethane Foam	(34 gm/m <sup>2</sup> )	0.24	$2.07 \times 10^{-5}$	1.0
	Nylon		0.4	$3.31 \times 10^{-5}$	
Structural	Fiber B	$128.5 \times 10^{-9}$	0.4	$3.98 \times 10^{-4}$	
Pressure	Nylon	(34 gm/m <sup>2</sup> )	0.4	$3.31 \times 10^{-4}$	
	Capran				0.00127
	Capran	$321 \times 10^{-9}$		$6.62 \times 10^{-4}$	0.00127
	EPT Foam				0.238
	Capran				0.00127
	Capran	(34 gm/m <sup>2</sup> )	0.4	$3.31 \times 10^{-4}$	0.00127
	Nylon				
	Aluminum Foil				0.0089

1. All fabric components are given in weight per unit area (area density)
2. EPT Foam = ethylene propylene terpolymer (Rubatex R-481-T)

Table VI. Estimated Weight Breakdown

Item	Weight (Kg)	
	Test Unit	Flight Unit (Est.)
Rings (8)	161.587	121.0
Clamp Rings (8)	63.503	44.6
Fairleads and Snap Rings (8)	5.008	5.0
Clamp Ring Bolts (24)	3.937	2.7
Cover Clamps (8)	6.432	6.4
Seal Clamps and Hardware	19.323	17.5
Cover Clamps - End (2)	1.751	1.7
Composite Cover- 31.9 SOM (343 Sq Ft)	59.103	59.1
Cables	31.978	31.9
Pulley Brackets (20)	23.587	17.5
Pulley (20)	24.403	19.0
Pulley Fittings and Hardware	15.476	15.0
Cable Terminals and Hardware	1.633	1.6
Total Weight	417.721	343.0
	(920.92)	(756.2)

## SECTION V

### CONCLUSIONS AND RECOMMENDATIONS

During the study program, many design concepts were reviewed and the cable supported tunnel was selected as the concept which best fulfills the design requirements. A 1/4-scale model was designed, fabricated and tested thus demonstrating the feasibility of the concept. A preliminary design and analysis was completed for a full-size ground test model of the cable supported tunnel. The preliminary design indicated that a space shuttle tunnel would meet the following requirements:

- (1) Deploy straight or in a 90-degree curved arc.
- (2) Maintain stability during and after deployment at any position from packaged to full deployment with  $1.027 \times 10^5$  Newtons/square meter (14.9 psi) internal gage pressure.
- (3) Maintain stability during and after deployment at any position from packaged to full deployment with near zero internal gage pressure.
- (4) Withstand the expected load conditions during all operations including orbit abort, re-entry and module deployment with a factor of safety of 3. (During crash landing, the factor of safety will be equal to or greater than 1.)
- (5) Provide an access to the payload during all phases of the mission with a tunnel diameter of at least 1.22 meters (48 inches).
- (6) Withstand all expected environmental conditions.
- (7) Utilize flexible materials which are either state-of-the-art or near state-of-the-art.
- (8) Utilize non-toxic, self-extinguishing or flame-retarding materials.
- (9) Deploy or retract at least 200 cycles.
- (10) Function at any altitude from sea level to 833,400 meters (450 nautical miles).

The study, model and preliminary design conducted during this program indicated the feasibility of the cable supported tunnel concept. It is recommended that a follow-on program be initiated in the near future which would provide for the detail design, fabrication and test of the full-scale ground-test model of the tunnel. The results obtained during the follow-on program would assist in establishing the interface requirements for both the space shuttle and sortie lab during their early design phases.

## APPENDIX I

### STRUCTURAL ANALYSIS

#### A. GENERAL

The structural analysis as presented herein follows accepted methods and procedures.

A review of the specified G loads shows that they are generally small when compared to the pressure loads. Consequently they should have little effect upon the design.

The crash landing condition occurs when the tunnel pressure differential is small and consequently the pressure loads are small. Only the longitudinal G in the crash landing condition produces higher ultimate G's than the other specified conditions. In the -8.0 G crash landing, the forces caused by the forward motion of the rings on the cables will have to be absorbed by bumpers placed on the rings to absorb the energy.

The 145 db acoustic environment will not be critical. Failure due to acoustic random noise is caused by fatigue failure due to bending stresses encountered at the structural natural frequencies. Since the natural frequency of the fabric is low and since the fabric acts as a membrane rather than a plate in bending, the number of cycles and the stress levels will be low. 145 db is equivalent to a dynamic pressure of  $345 \text{ N/meter}^2$  (0.05 psi) above ambient, a low stress when compared to the limit design stress of  $1.027 \times 10^5 \text{ N/m}^2$  (14.9 psi).

#### B. RING

##### 1. Loading Conditions

The ring structure consists of a steel tube to which the structural fabric is clamped by a sectionalized steel clamp. The micrometeoroid blanket is clamped to the rings by use of a second clamp.

The principal function of the ring structure is to resist the hoop tension produced by the internal pressure. When the tunnel is in the rotated position the rings also transfer to the cables the loads which act radial to the axis of rotation of the tunnel. These radial loads subject the ring to bending loads as well as hoop tension loads.

TABLE A-1

CRITICAL LOADING CONDITIONS FOR RING

	LOADING CONDITION	TUNNEL POSITION	G LOADS			PRESSURE DIFFERENTIAL		TEMP. RANGE				CRITICAL STRUCTURE
			X	Y	Z	PSI	NEW/M <sup>2</sup>	FAHR.		KELVIN		
								MAX	MIN	MAX	MIN	
A	REENTRY	STRAIGHT-EXTENDED	1.4	0.7	4.0	14.9	102,730	-100	200	200	366	CLAMP TENSION
B	REENTRY	ROTATED-EXTENDED	1.4	0.7	4.0	14.9	102,730	-100	200	200	366	RING BENDING
C	ORBIT ABORT	STRAIGHT	-4.5	1.0	1.20	0	0	-100	150	200	366	RING COMPRESSION

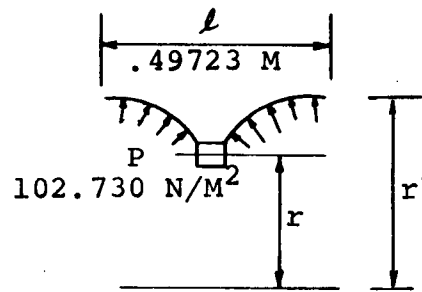


Figure 1

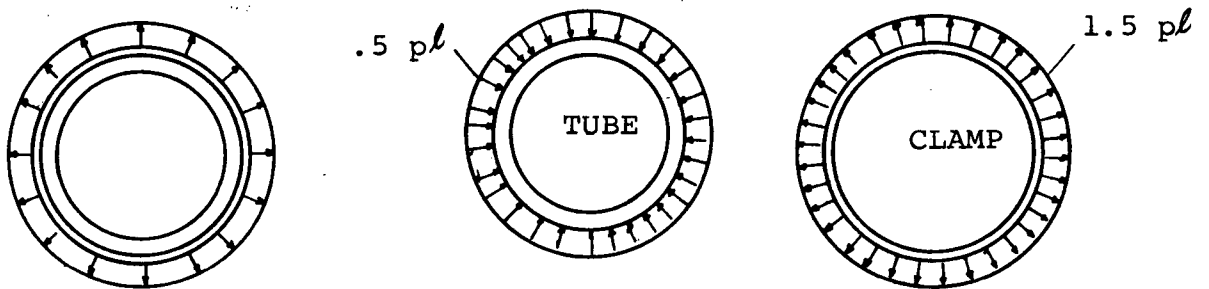


Figure 2

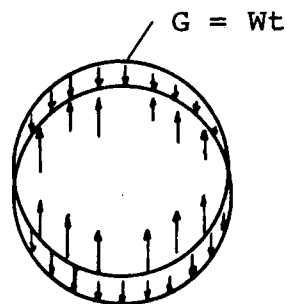


Figure 3



The clamp will be pretensioned sufficiently so that when subjected to the maximum limit load it will have a positive clamping action on the fabric. The pretension will be set so that the clamping force will be equal to 50% of the maximum limit radial force when the ring is subjected to the limit load.

From the above, it is apparent that three loading conditions should be investigated; one which produces the maximum hoop tension in the clamp, one which produces maximum bending in the ring tube and one which produces maximum hoop compression in the tube.

The maximum hoop tension will occur when the ring is in its straight fully extended position and subjected to its maximum tunnel pressure differential. From a review of the requirements it is apparent that the maximum hoop tension will occur in the reentry condition with the tunnel extended.

The maximum bending in the tubular ring will occur in the module deployment condition with the tunnel fully deployed.

The maximum hoop compression in the tube will occur when there is no tunnel pressure differential. This would occur in the orbit abort condition.

In addition to the pressure loads the ring is also subjected to the various G loads listed in the requirements. The magnitude of the stresses produced by the G loads will be small compared to the pressure and prestress clamping loads. The maximum G's when the tunnel is subjected to the maximum differential pressure occurs in the re-entry condition. The maximum G's for the minimum pressure condition which subjects the tubular section of the ring to compression occurs in the orbit abort condition.

The three loading conditions for which the ring will be analyzed are summarized in Table A-1.

## 2. Loads

### a. Condition A - Reentry

#### (1) Pressure Loads

In condition A the limit pressure load on the ring will be a uniform load. The axial load  $F$  produced by the pressure load will be

$$F_p = p l r' \quad (\text{Ref Figure 1})$$

From statics reference Figure 4, the load on the ring is

$$w = p(2H + T) \times \frac{(r + \Delta r)}{r - A/2}$$

For angles of  $\phi$  up to values of  $\pi/2$ , knowing  $B$ ,  $\theta$ ,  $r$  and the fabric length  $s$ , the value of  $H$  can be determined from the following formulas

$$H = [(B + r \cos \alpha) \cos \theta - R \cos \phi \cos \alpha \cos \theta] \sin \theta$$

$$\phi = s/2R$$

$$c = 2R \sin \phi = 2(B + r \cos \alpha) \sin \theta$$

$$\frac{c}{s} = \frac{\sin \phi}{\phi}$$

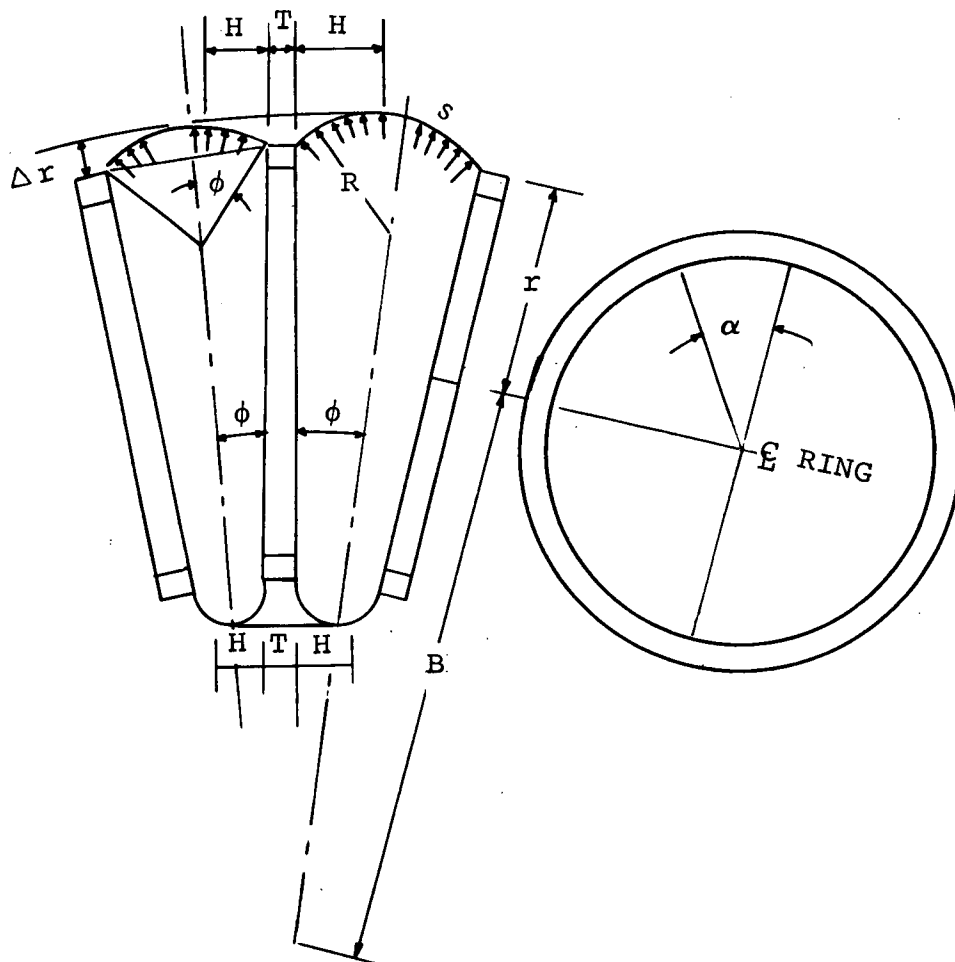


Figure 5.

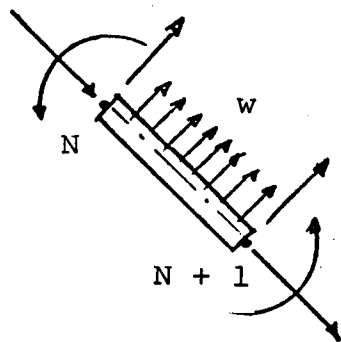
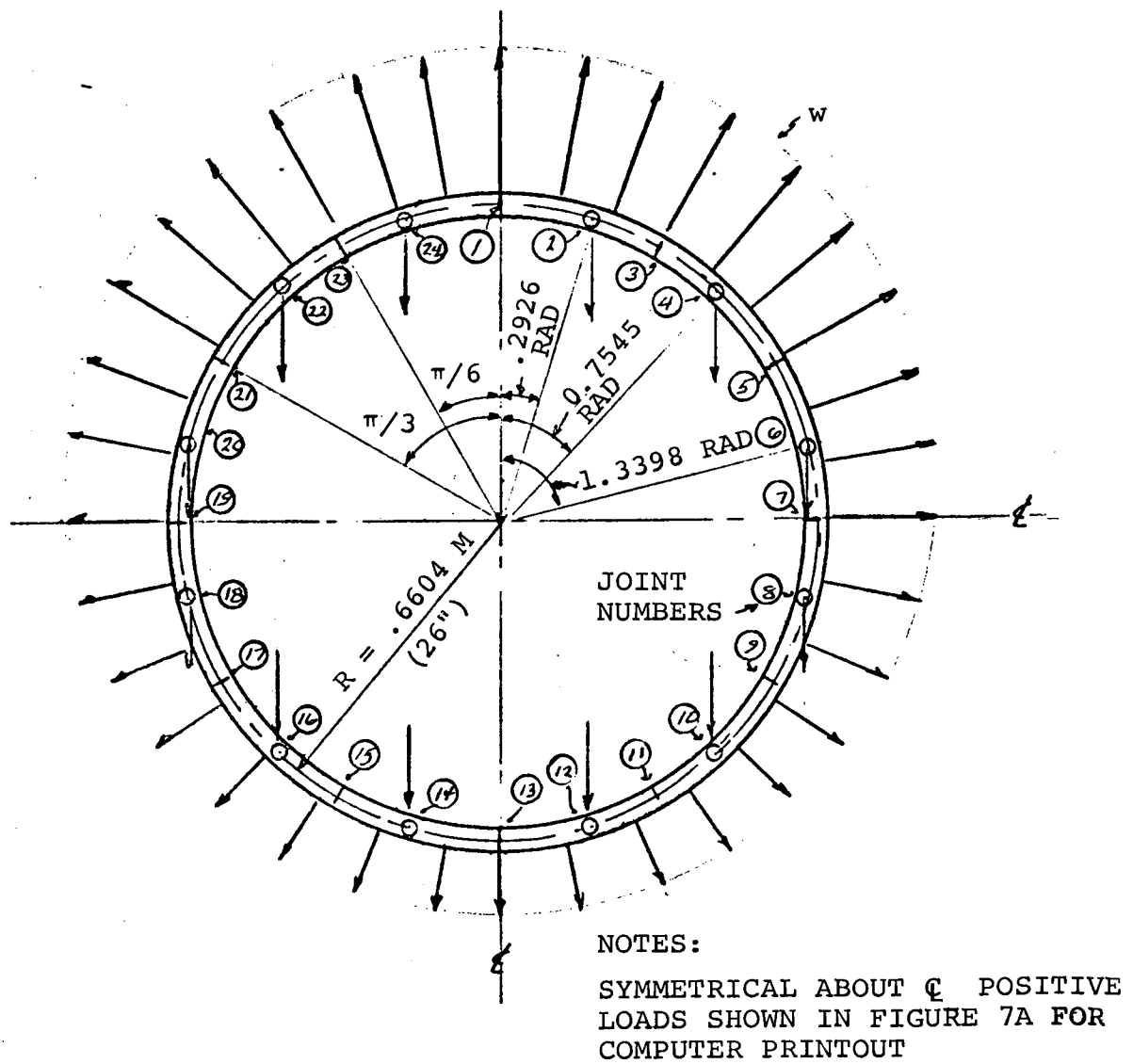


Figure 6



RING EXTERNAL LOADS  
 CONDITION B ROTATED TUNNEL

Figure 7

TABLE A-2

ULTIMATE RING LOADS - CONDITION B - TUNNEL ROTATED  
(FACTOR OF SAFETY OF 3 INCLUDED)

MEMBER	JOINT	AXIAL FORCE NEWTONS	SHEAR FORCE NEWTONS	MOMENT NEWTON METERS
1	1	-103,483	-15,235	-1423.0
1	2	+103,483	-17,283	1620.1
2	2	-101,327	-17,295	-1620.3
2	3	+101,327	- 8,375	942.3
3	3	-100,587	-15,056	- 942.3
3	4	+100,587	-10,455	595.8
4	4	- 93,697	-20,802	- 595.9
4	5	+ 93,697	-10,664	- 361.9
5	5	- 92,795	-16,799	361.6
5	6	+ 92,795	-13,246	- 674.5
6	6	- 85,266	-12,134	674.4
6	7	+ 85,266	-10,054	- 810.9
7	7	- 85,278	- 9,715	810.9
7	8	+ 85,278	-10,749	- 710.0
8	8	- 77,865	- 8,807	710.0
8	9	+ 77,865	-14,465	- 116.7
9	9	- 78,718	- 8,592	116.8
9	10	+ 78,718	-11,668	226.4
10	10	- 74,377	- 2,811	- 226.2
10	11	+ 74,377	-11,397	897.4
11	11	- 75,015	- 5,959	- 897.3
11	12	+ 75,015	- 7,092	995.5
12	12	- 73,149	- 4,808	- 995.7
12	13	+ 73,149	-10,769	1580.4
13	13	- 73,144	- 7,838	-1580.2
13	14	+ 73,144	- 4,794	992.7
14	14	- 75,006	- 7,096	- 992.3
14	15	+ 75,006	- 5,955	893.6
15	15	- 74,362	-11,381	- 893.0
15	16	+ 74,362	- 2,827	224.3
16	16	- 78,709	-11,651	- 224.2
16	17	+ 78,709	- 8,609	- 115.9
17	17	- 77,848	-14,450	115.9
17	18	+ 77,848	-88,226	- 706.3
18	18	- 85,264	-10,730	706.3
18	19	85,264	- 9,734	- 804.2
19	19	- 85,238	-10,083	804.2
19	20	85,238	-12,100	- 672.1
20	20	- 92,756	-13,270	672.1
20	21	+ 92,756	-16,775	- 363.8
21	21	- 93,654	-10,679	363.8
21	22	93,654	-20,788	591.2
22	22	-100,528	-10,456	- 591.1
22	23	100,528	-15,055	937.5
23	23	-101,305	- 8,368	- 937.3
23	24	101,305	-17,302	1616.4
24	24	-103,467	-17,263	-1616.3
24	1	103,467	-15,255	1473.0

FIG 8

ULTIMATE RADIAL LOADS ON RING  
CONDITION B - ROTATED TUNNEL

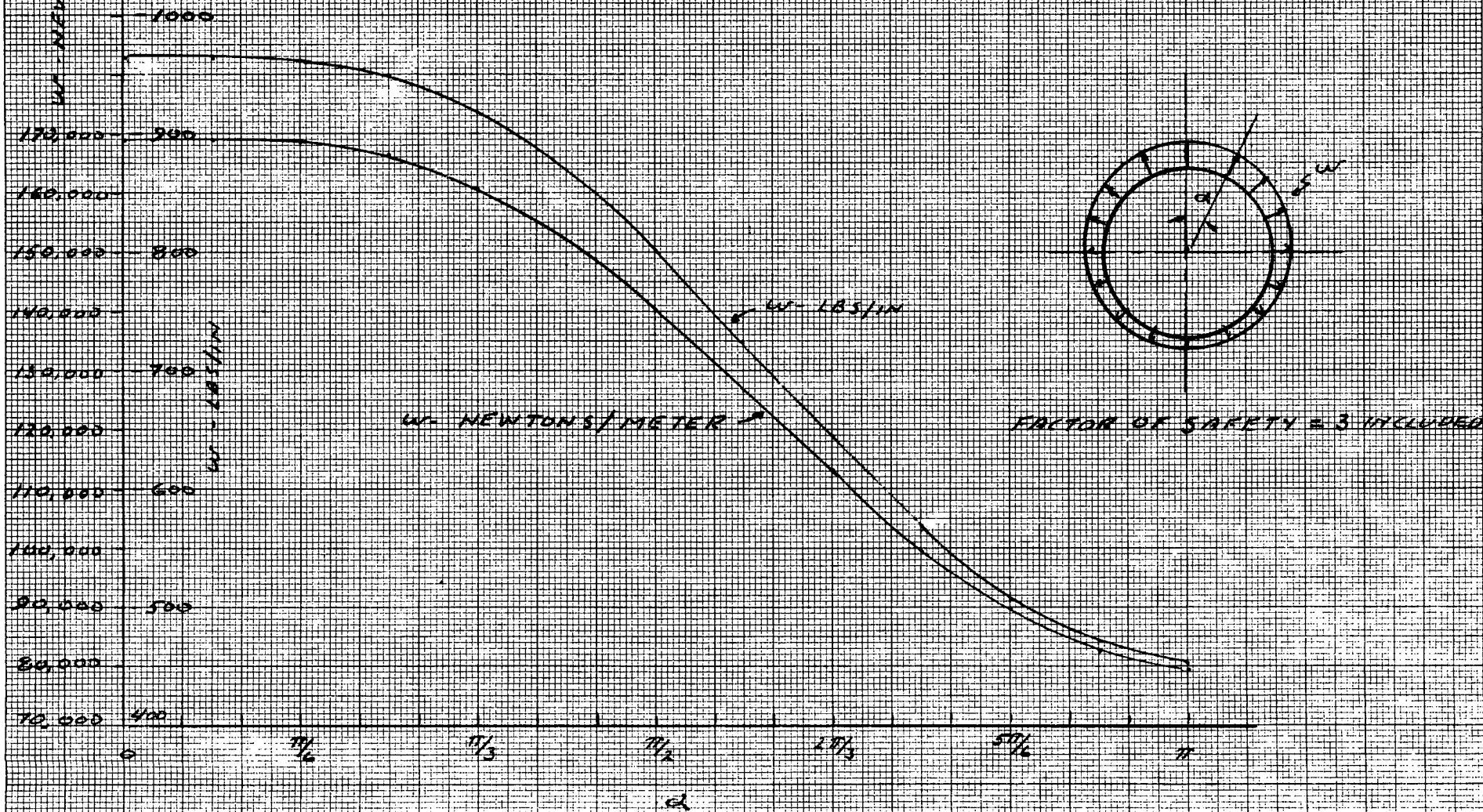
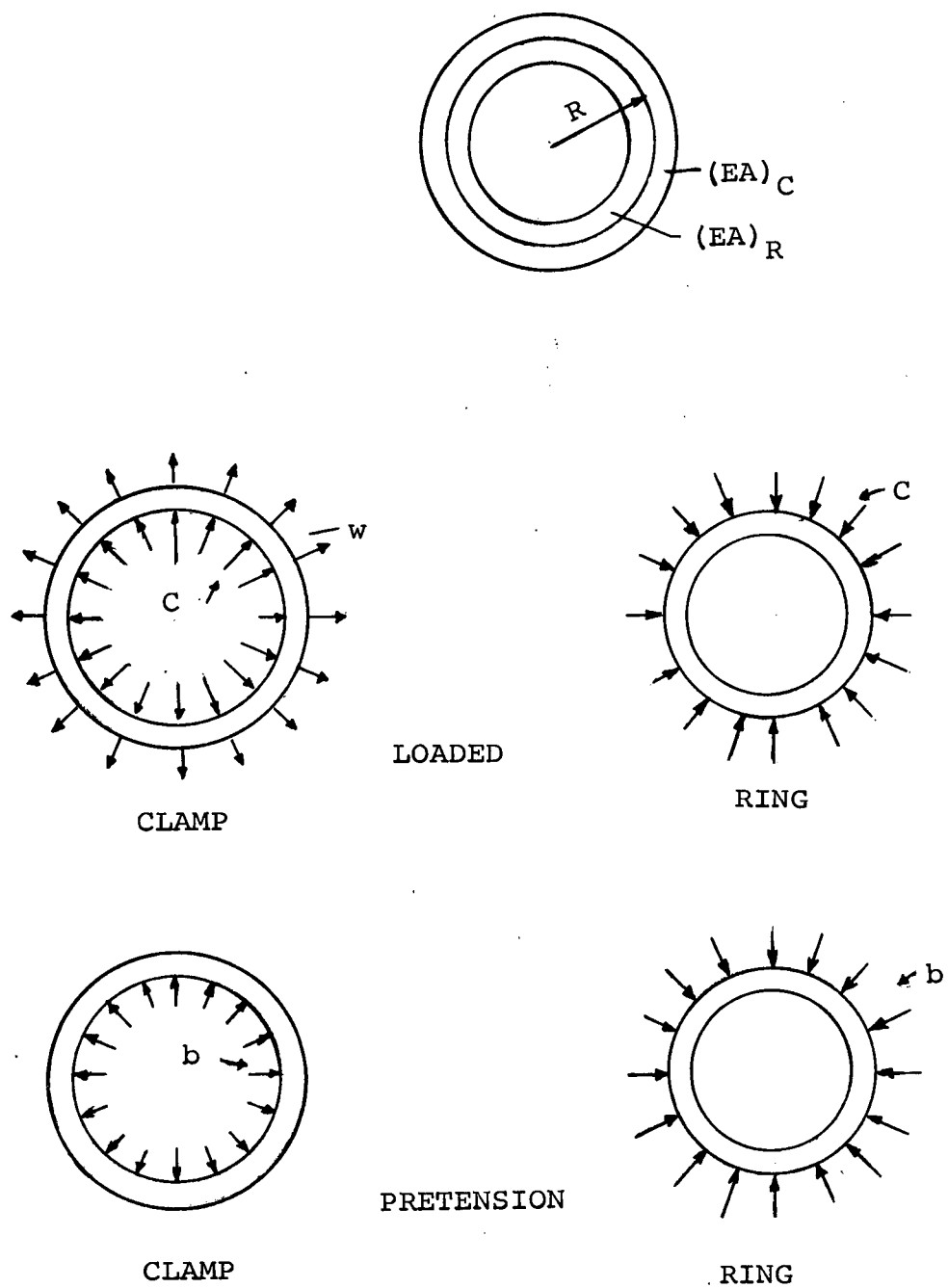


TABLE A-3

SPACE SHUTTLE CREW TRANSFER TUNNEL RING FRAMES  
 ULTIMATE RING LOADS - CONDITION B - TUNNEL ROTATED  
 (FACTOR OF SAFETY OF 3 INCLUDED)

MEMBER FORCES				
MEMBER	JOINT	AXIAL FORCE (LBS)	SHEAR FORCE (LBS)	MOMENT (IN LBS)
1	1	-23264.094	-3425.035	-12594.54
1	2	23264.094	-3885.285	14339.11
2	2	-22779.734	-3888.102	-14340.55
2	3	22779.734	-1882.852	8339.95
3	3	-22612.902	-3384.751	-8340.33
3	4	22612.902	-2350.421	5273.32
4	4	-21063.891	-4676.508	-5274.18
4	5	21063.891	-2397.418	-3203.50
5	5	-20861.148	-3776.660	3200.26
5	6	20861.148	-2977.840	-5970.10
6	6	-19168.477	-2726.750	5969.05
6	7	19168.477	-2260.270	-7176.91
7	7	-19171.242	-2184.094	7177.12
7	8	19171.242	-2416.453	-6284.72
8	8	-17504.848	-1979.937	6284.53
8	9	17504.848	-3251.871	-1033.01
9	9	-17696.449	-1931.640	1033.56
9	10	17696.449	-2623.106	2004.36
10	10	-16720.719	-632.049	-2002.45
10	11	16720.719	-2562.058	7942.52
11	11	-16863.992	-1339.664	-7941.83
11	12	16863.992	-1594.349	8810.50
12	12	-16444.582	-1080.982	-8812.41
12	13	16444.582	-2421.044	13988.16
13	13	-16443.367	-2424.291	-13986.33
13	14	16443.367	-1077.735	8785.97
14	14	-16862.148	-1595.216	-8782.59
14	15	16862.148	-1338.797	7908.74
15	15	-16717.340	-2558.618	-7904.24
15	16	16717.340	-635.489	1984.80
16	16	-17694.520	-2619.361	-1984.00
16	17	17694.520	-1935.385	-1025.56
17	17	-17500.930	-3248.406	1025.91
17	18	17500.930	-1983.402	-6251.16
18	18	-19168.934	-2412.187	6250.98
18	19	19168.934	-2188.359	-7117.80
19	19	-19162.289	-2266.801	7117.59
19	20	19162.289	-2720.219	-5948.87
20	20	-20852.371	-2983.254	5948.75
20	21	20852.371	-3771.246	-3219.93
21	21	-21054.270	-2400.698	3220.11
21	22	21054.270	-4673.227	5232.73
22	22	-22599.699	-2350.632	-5231.72
22	23	22599.699	-3384.540	8297.47
23	23	-22774.199	-1881.207	-8295.77
23	24	22774.199	-3889.746	14306.22
24	24	-23260.207	-3880.844	-14305.36
24	1	23260.207	-3429.477	12594.46



CONDITION C - ORBIT ABORT

Figure 9

When the fabric lobes contact each other the determination of H by analytical means becomes difficult. Consequently, graphical methods are used when  $\phi > \pi/2$ . Values of  $\Delta r$  were also obtained graphically.

The ring loading so obtained is given in Figure 8. Having the ring loading and geometry the ring was analyzed on a digital computer employing the STRESS program. The output of this program is given in Tables A2 and A3. The loads presented in these tables contain the factor of safety of 3 and are therefore ultimate loads.

## (2) G Loads

The G loads will be reacted in this condition in the same manner as in condition A.

### c. Condition C - Orbit Abort

Since the tunnel is covered by a micrometeoroid blanket, it will be assumed in this analysis that there is no temperature gradient in the ring.

The required clamping force is derived below.  
(Reference Figure 9)

In the loaded condition the rings are in contact and exert upon each other a uniform radial force  $c$ . The radial load acting on the clamp would be  $(w + c)$  acting outward and the radial load acting on the tube would be  $c$  acting inward.

The radial deflection at the interface R of the clamp and the tube from the loaded condition to the unloaded condition prior to assembly would be

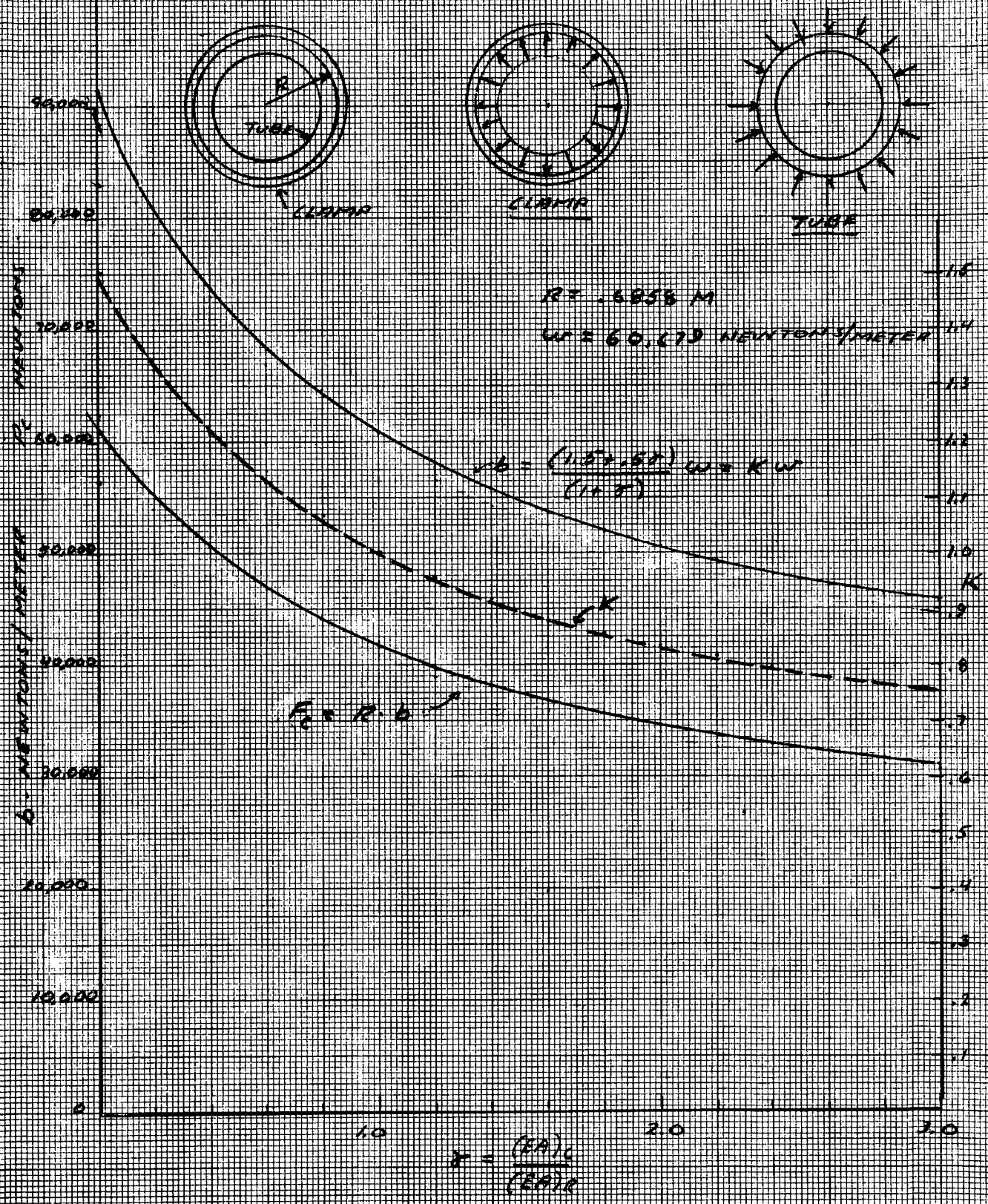
$$\Delta c_o = \frac{(w + c)}{(EA)_c} \cdot R^2 \quad (\text{radially inward})$$

$$\Delta R_o = \frac{c}{(EA)_c} \cdot R^2 \quad (\text{radially outward})$$

The difference of the above deflections is

$$\Delta c_o + \Delta R_o = \frac{(w + c)}{(EA)_c} R^2 + \frac{c}{(EA)_R} \cdot R^2$$

FIG 10  
LIMIT PRETENSION LOADS



PREPARED BLC

GOODYEAR AEROSPACE

PAGE

CHECKED

CORPORATION

MODEL

DATE

GER-

REV DATE

CODE IDENT

25500

d. Ring Analysis

LOCATIONS OF CABLE RESTRAINT POINTS, AND  
RING ELEMENTS.

REF. DWG. 72 Q5 222B

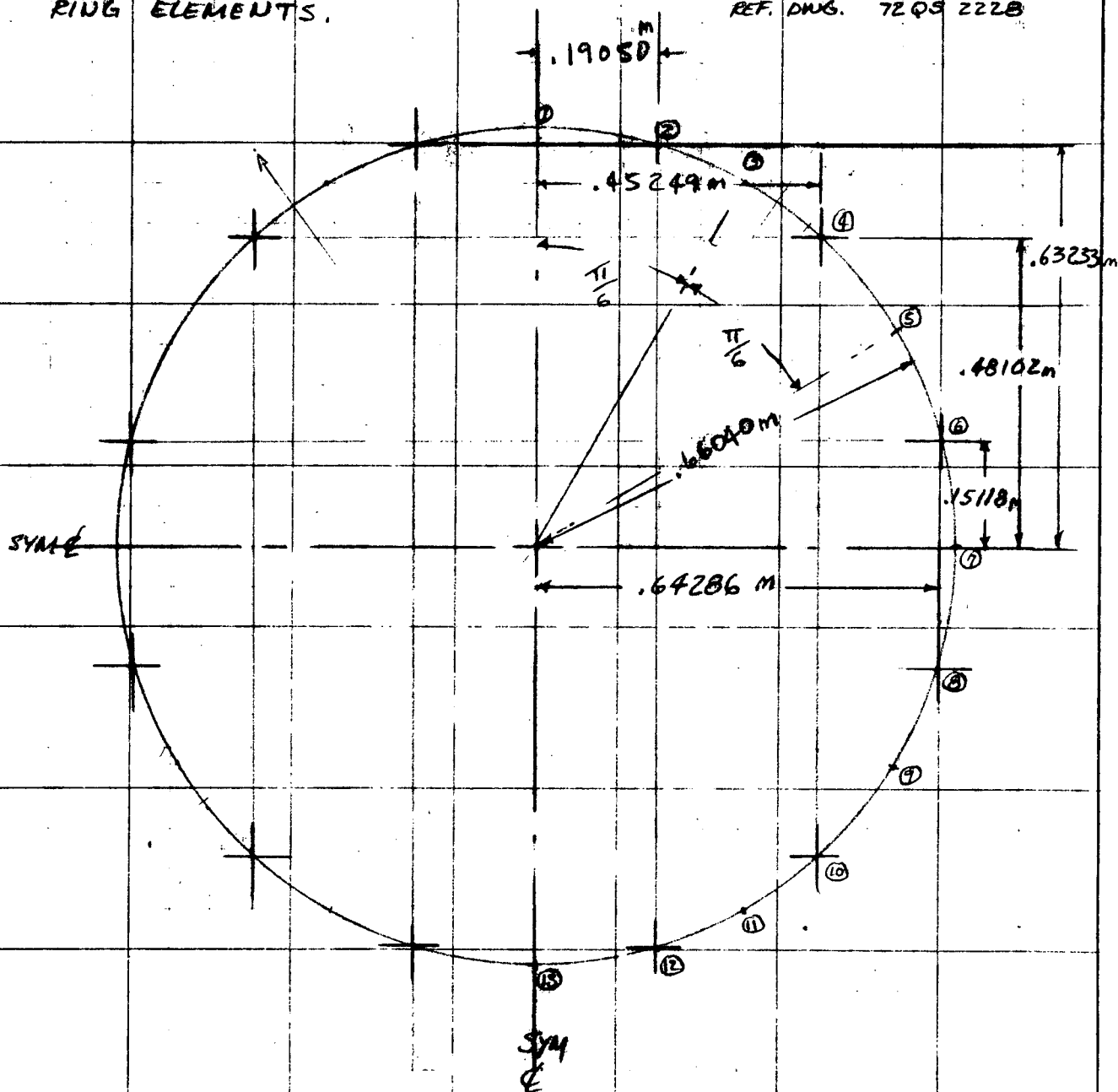


FIG 11

CHECKED

CORPORATION

MODEL

DATE

GER-

REV DATE

CODE IDENT

25500

## (1) Section Properties

CLAMP  
SECTION, AREA, AND C.G. LOCATION

REF. DWG. 72 QS 2228

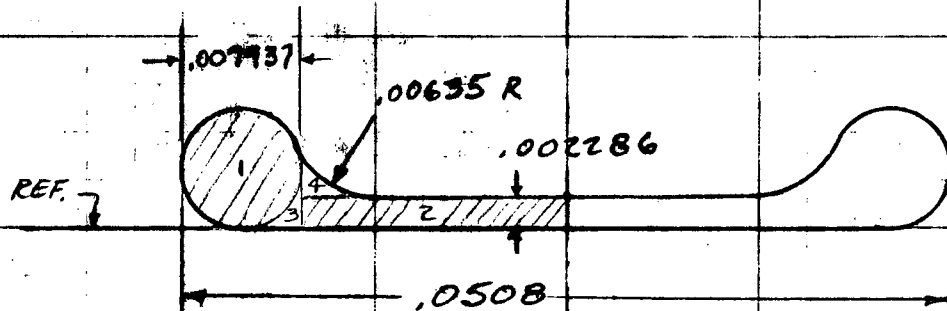


FIG 12

CLAMP CROSS-SECTION

2X SIZE

PROP. 1/2 CLAMP

ITEM AREA

Y

1	.000049477	.0039687
2	.000039920	.0011430
3	.000003381	.0008867
4	.000004303	.0030988

$$A = 2(.000097081) = .00019416 \text{ m}^2 \quad (.3009 \text{ in.}^2)$$

$$\frac{1}{2} \sum Ay = .25832 \times 10^{-6}$$

$$\bar{y} = \frac{.25832 \times 10^{-6}}{.97081 \times 10^{-4}} = .00266 \text{ m} \quad (.1047 \text{ in.})$$

$$I_y = .0586 \times 10^{-6} \text{ m}^4 \quad (.1407 \text{ in.}^4)$$

PREPARED BLC

GOODYEAR AEROSPACE

PAGE

CHECKED

CORPORATION

MODEL

DATE

GER-

REV DATE

CODE IDENT

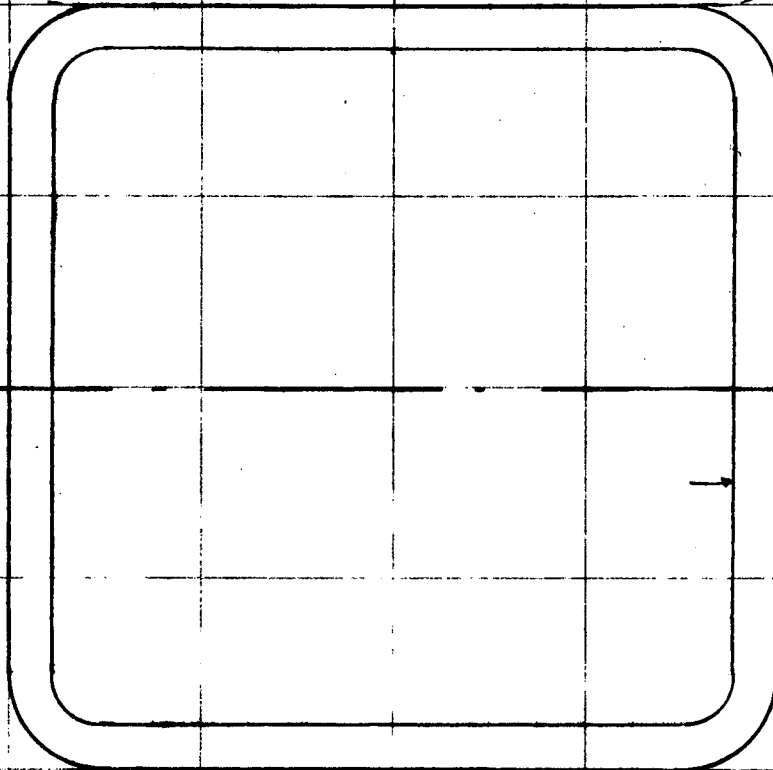
25500

## RING ANALYSIS

RING SECTION

REF. DWG. 72 Q5 2228

FIG 13

.003048  
m..0508 X .0508 X .003 WALL SQUARE  
TUBE 2 X SIZE

$$AREA = \underline{.0005503 \text{ m}^2} \quad (.8530 \text{ IN.}^2)$$

$$I = \underline{.20224 \times 10^{-6} \text{ m}^4} \quad (.4859 \text{ IN.}^4)$$

$$J = \frac{4A^2}{\sum \frac{ds}{r}} = \underline{.34085 \times 10^{-6} \text{ m}^4} \quad (.8189 \text{ IN.}^4)$$

(2) Preload

## RING ANALYSIS

CALCULATION OF REQUIRED CLAMP PRELOAD  
IN ORDER THAT  $1/2$  THE LIMIT PRESSURE ON  
THE RING REMAIN, AT THE MAXIMUM  
LOAD CONDITION. (REF PAR. B-2-C)

$$\frac{\text{AREA CLAMP}}{\text{AREA RING}} = \frac{.00019416}{.0005503} = .3528$$

$$k = \left( \frac{1.5 + .5 \left( \frac{A_c}{A_r} \right)}{1 + \left( \frac{A_c}{A_r} \right)} \right)$$

$$k = \frac{1.6764}{1.3528} = 1.2392$$

CLAMP PRELOAD THEN MUST EQUAL:

$$P_c = k p R L$$

WHERE  $k$  IS INTENSITY FACTOR

$p$  IS APPLIED PRESSURE, =  $102,730 \text{ N/m}^2$  (14.9  $\text{lb/in}^2$ )

$R$  IS RADIUS = .81468 m.

$L$  IS LENGTH = .49723 m.

$$P_c = 1.2392 \times 102,730 \times .81468 \times .49723$$

$$P_c = \underline{51568 \text{ N.}} \quad (11593 \text{ LB.})$$

(3) Clamp

## RING ANALYSIS

CHECK MAXIMUM HOOP TENSION IN CLAMP.

$P_c = 51568 \text{ N}$ . PRELOAD,  $\neq$  SINCE PRESSURE LOAD  
ADDS DIRECTLY TO CLAMP IN RATIO TO ITS AREA,  
TO TOTAL AREA OF RING  $\neq$  CLAMP,

$$P_L = 102,730 \times 1.81468 \times .49723 \times \frac{.00019416}{.00074446} = 10853 \text{ N}$$

$$f_t, \text{ CLAMP STRESS} = \frac{P_c + P_L}{A_c}$$

$$\text{LIMIT } f_t = \frac{62421 \text{ N}}{.00019416 \text{ m}^2} = 321.493 \times 10^6 \text{ N/m}^2 \quad (46,629 \text{ LB/IN}^2)$$

$$f_{t \text{ ULT.}} = 3 \times 321.493 \times 10^6 = 964,479 \times 10^6 \text{ N/m}^2, \text{ ULT. TENSION.}$$

$$(139,886 \text{ LB/IN}^2 \text{ ULT.})$$

$$\text{ALLOWABLE TENSION} = 1034.2 \times 10^6 \text{ N/m}^2 \quad (150,000 \text{ LB/IN}^2)$$

$$M.S. = \frac{1034.2}{964.48} - 1 = \underline{.07}$$

AN INVESTIGATION OF THE RING LOADS DUE TO G FORCES  
ON RE-ENTRY INDICATES THAT THE MAXIMUM ADDED TENSION  
WHICH THE CLAMP BAND WOULD SUSTAIN IS (LIMIT LOADS)

$$\text{ADDED } P_L = 67.30 \text{ N}, \quad (15.13 \text{ LB})$$

THIS ADDITIONAL LOAD IS NEGLIGIBLE - SINCE IT  
ADDS ONLY .108% TO THE LIMIT LOAD

## (4) Stability

## RING ANALYSIS

CHECK STABILITY OF RING COMPRESSION MEMBER UNDER PRELOAD: FOR BUCKLING FORMULAS SEE REF. 6 PG. 873.

$$P_R = 51568 \text{ N.}$$

$$w = \frac{P_R}{r} = \frac{51568 \text{ N.}}{.6608 \text{ m}} = 78086 \text{ N/m LIMIT.}$$

$$\text{CRITICAL PRESSURE } p' = \frac{3EI}{r^3}, \text{ BUCKLING IN PLANE}$$

$$p' = \frac{3 \times 199.948 \times 10^9 \times .20224 \times 10^{-6}}{(.6604)^3} = 421,200 \text{ N/m.}$$

IN PLANE

$$\text{CRITICAL PRESSURE } p' = \frac{9EI}{r^3 \left(4 + \frac{EI}{\omega}\right)}, \text{ BUCKLING OUT OF PLANE (INCLUDE I OF CLAMP)}$$

$$p' = \frac{9 \times 199.948 \times 10^9 \times (.20224 \times 10^{-6} + .0586 \times 10^{-6})}{(.6604)^3 \left(4 + \frac{199.948 \times 10^9 \times .26084 \times 10^{-6}}{75.842 \times 10^9 \times .34085 \times 10^{-6}}\right)} = 270,830 \text{ N/m}$$

OUT PLANE

$$w_{ULT.} = 234,258 \text{ N/m}, \text{ M.S.} = \frac{270,830}{234,258} - 1 = .15$$

## (5) Tube

CHECK CRITICAL LOAD IN RING FOR MODULE DEPLOYMENT (AT POINT ② OF RING)

$$P_R = 51568 \text{ N (PRELOAD)}$$

THE LIMIT TENSION LOAD IN THE CLAMP DUE TO THE COMBINED PRESSURE & CABLE REACTIONS ON THE RING & CLAMP IS:

$$C = \frac{A_c}{A_c + A_R} \left( \frac{\text{ULT. AXIAL FORCE}}{3} \right) = \frac{.00019416 \left( \frac{103483}{3} \right)}{.00074446} = 8996.3 \text{ N.}$$

MOMENT EFFECT OF CLAMP ECCENTRICITY =

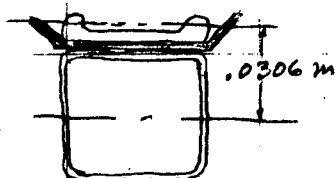


FIG 14

$$8996.3 \text{ N.} \times .0306 \text{ m} = 275.28 \text{ Nm}$$

$$\text{LIMIT TENSION LOAD IN RING} = \frac{.0005503 \left( \frac{103483}{3} \right)}{.00074446} = 25498 \text{ N.}$$

## RING ANALYSIS

## CRITICAL RING BENDING (CONT.)

RING BENDING (FROM COMPUTER ANAL.)

$$M_R = \frac{1620.1}{3} = 540.03 \text{ Nm, LIMIT}$$

(COMP. OF OUTER RIM)

$$\text{TOTAL } M_R = 540.03 + 275.28 = \underline{815.31} \text{ Nm}$$

## CRITICAL COMPRESSIVE STRESS IN RING

$$f_c = \frac{P}{A} + \frac{Mc}{I}, \text{ (USING AVERAGE BENDING STRESS IN MAX. LOADED TUBE WALL)}$$

$$f_c = \frac{51568 - 25498}{.0005503} + \frac{815.31 \times .023876}{.20224 \times 10^{-6}}$$

$$f_c = 47.374 \times 10^6 + 96.257 \times 10^6 = \underline{143.63 \times 10^6} \text{ N/m}^2 \text{ COMP.}$$

$$= (20,832. \text{ LB/IN.}^2)$$

$$f_{c \text{ ULT.}} = 3 \times 143.63 \times 10^6 = 430.89 \times 10^6 \text{ N/m}^2$$

FOR NORMALIZED 4130 STEEL : (FROM SUMMER/LL TUBING

$$f_c \text{ ALLOWABLE} = 461.95 \times 10^6 \frac{\text{DATA}}{\text{N/m}^2} = (67000 \text{ LB/IN.}^2)$$

$$M.S. = \frac{461.95}{430.89} - 1 = \underline{.07}$$

INVESTIGATING THE RING FOR LOADS IMPOSED BY A 95 PERCENTILE MAN, 91.13 kg. (200.9 lb.) WITH 1.2 G IN ALL 3 VEHICLE AXES, INDICATES AN INCREASE IN TENSION

IN THE RING OF 96.93 N. (21.79 LB.) AND OF 14.02 NM (124.06 IN. LB.) IN THE MOMENT, (WITH THE MOMENT ADDING TO THE ABOVE COMPRESSION STRESS RESULTS) THE CHANGE IN COMPRESSION STRESS IS CALCULATED AS 1.06 %.

The preload will deflect the clamp from the no-load condition an amount

$$\Delta c = \frac{bR^2}{(EA)_c}$$

Similarly

$$\Delta R = \frac{bR^2}{(EA)_R}$$

When assembled, it follows from continuity that

$$\Delta c_o + \Delta R_o = \Delta c + \Delta R$$

$$\frac{(w + c)}{(EA)_c} \cdot R^2 + \frac{c}{(EA)_R} \cdot R^2 = \frac{bR^2}{(EA)_c} + \frac{bR^2}{(EA)_R}$$

$$\frac{(w + c)(EA)_R + c(EA)_c}{(EA)_c \times (EA)_R} = b \left[ \frac{(EA)_c + (EA)_R}{(EA)_c \times (EA)_R} \right]$$

$$b = \frac{(w + c)(EA)_R + c(EA)_c}{(EA)_c + (EA)_R}$$

$$b = \frac{(w + c) + c \cdot \frac{(EA)_c}{(EA)_R}}{1 + \frac{(EA)_c}{(EA)_R}}$$

Let

$$\frac{(EA)_c}{(EA)_R} = \gamma, \quad c = .5w$$

Then

$$b = \left[ \frac{1.5 + .5\gamma}{1 + \gamma} \right] w$$

The axial tension load in the clamp would equal the axial compression load in the tube and can be obtained from

$$F = bR.$$

Values of b and F have been determined for a range of values of  $\gamma$  and are plotted in Figure 10.

$$w = p \cdot l \cdot \frac{R'}{R} \quad (\text{Reference Figure 17})$$

$$w = 102,730 \times .49723 \times \frac{.81468}{.6858} = 60,679 \text{ Newtons/Meter}$$

## C. CABLES

### 1. Loading Conditions

The primary structural function of the cables is to resist the longitudinal pressure force acting on the cross sectional area of the tunnel. This pressure force is equal to the product of the pressure and the cross sectional area of the tunnel. This force is resisted in part by the tension in the cables and in part by the longitudinal tension in the fabric. Consequently, the maximum tension in the cables will occur when the tunnel cross-sectional area is a maximum and the tension in the fabric is a minimum. This occurs when the tunnel is fully retracted since in this condition the fabric tension is almost nil and the tunnel diameter is at a maximum.

A secondary function of the cables is to resist the lateral side loads caused by the G effects. When the tunnel has a high differential pressure the maximum lateral G's occur in the reentry condition at which time the  $G_y = .7$  and the  $G_z = 4.0$  giving a resulting G of  $(.7^2 + 4.0^2)^{1/2} = 4.06$  G.

The tension in the cable resulting from a uniform side load can be obtained by trial from the following equation:

$$T = \frac{wL}{2} \sqrt{\frac{AE}{6(T-T_0)}} \quad (\text{Reference 7 Page 262})$$

Where  $T$  = Tension in the cable

$w$  = Uniform loading on the cable

$L$  = Cable length

$A$  = Area of cable

$E$  = Young's modulus of elasticity

$T_0$  = Initial tension in cable

Since  $wL$  equals the tunnel weight  $W$  the above expression can be modified by substituting  $W$  for  $wL$  in which case it is apparent that  $T$  is independent of  $L$

$$T = \frac{W}{2} \sqrt{\frac{AE}{6(T-T_0)}}$$

## 2. Cable Analysis

$$T_0 = \frac{\pi R^2 p}{N}$$

Where  $R$  = Radius

$p$  = Internal pressure

$N$  = Number of cables

102,730 NEWTON/SQ METER  
(14.9 PSI)

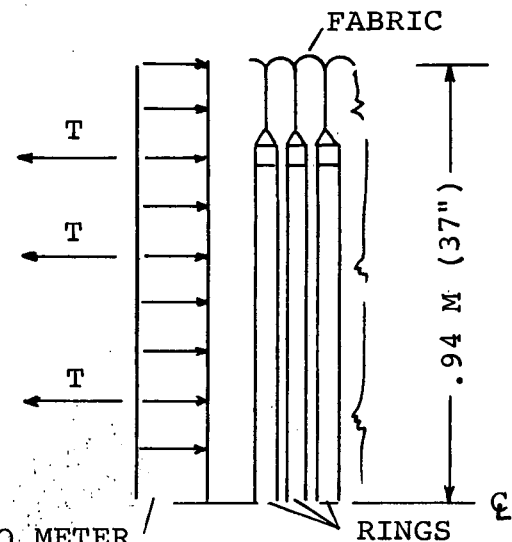


Figure 15

$$T_0 = \frac{\pi \times .94^2 \times 102,730}{12} = 23,700 \text{ Newtons} \cdot$$

(5350 lbs)

Assume mass tunnel = 340 kilograms (750 lbs)

$$\text{Then } W \text{ for each of the 12 cables} = \frac{340 \times G}{N} = \frac{340 \times 4.06}{12}$$

$$= 115 \text{ kilograms}$$

$$= 1130 \text{ Newtons (254 lbs)}$$

Twelve stainless steel cables .0111 M in dia. (7/16") will be used.

The EA of cables vary with load. Since a factor of safety of three is required, the cables will be loaded to one third of their ultimate load. Consequently, the EA at one third of the ultimate load will be used in this analysis. The EA was determined by extrapolating from tests reported in the John A Roebling's Sons Corporation Report "Elastic and Thermal Properties of Roebling Aircord) and was found to be  $6.11 \times 10^6$  Newtons (1,360,000 lbs).

Substituting in the formula

$$T = \frac{W}{2} \sqrt{\frac{AE}{6(T - T_0)}}$$

$$T = \frac{1130}{2} \sqrt{\frac{6,110,000}{6(T - 23,700)}}$$

Evaluating T by trial and error

Try  $T = 24,250$  Newtons (5590 lbs)

$$T = \frac{1130}{2} \sqrt{\frac{6,110,000}{6(24,250 - 23,700)}}$$

$$T = 24,300 \text{ Newtons (check)}$$

Ultimate strength of cable = 72,500 Newtons (16,300 lbs)  
(Ref. 8 Page 8.4.1.2 (a))

$$M.S. = \frac{72,500}{24,250 \times 3} - 1 = \underline{.00}$$

#### D. FABRIC

##### 1. Loading Conditions

The fabric is attached to the rings in such a manner that there is always excess fabric in the hoop direction. Consequently, there will be no hoop stresses in the fabric. The fabric stress in the longitudinal direction will be  $p \cdot R$  where  $p$  is the differential pressure between the inside and the outside of the fabric and  $R$  is the radius of the fabric. The maximum pressure has been specified as 102,730 Newtons/sq meter (14.9 psi). The maximum radius will occur when the tunnel is in its extended position.

In addition to the pressure loads, the fabric will be subjected to G loads. When in its maximum pressured condition the maximum G's occur in the reentry condition. The lateral G's will not affect the fabric since the loads resulting from these G's are transmitted from the rings to the cables. However, since the rings can move on the cables without restraint in the longitudinal direction, the longitudinal G load of 1.4 will have to be transmitted through the fabric. Assuming a tunnel mass of 340 kilograms, (750 lbs), the longitudinal G load would be  $1.4 \times 340 \times 9.806 = 4675$  Newtons.

## 2. Fabric Analysis

A fabric made from DuPont's Fiber B having a strength of 262,500 Newtons/Meter (1500 lbs/in) has been selected for use on the tunnel. This is a new fabric. Little test data is available on its strength under sustained load. Consequently more information is required in this area. A test program should be carried out to obtain the necessary test data. In this analysis a fabric factor of five instead of the specified factor of safety of three will be employed to take account of the effects of creep rupture. A fabric factor of five has been used successfully on airships.

From Figure 16 it is apparent that the high temperature strength of Fiber B is excellent. At the maximum specified tunnel temperature of 366° Kelvin the fabric retains 88% of its room temperature strength.

In the extended position of the tunnel the distance between rings is 0.446 meters (17.576 inch). The fabric length is 0.54 meters (21.25 inch) producing a radius of 0.2575 meters (10.148 inch).

The tension in the fabric at point A Figure 17 is

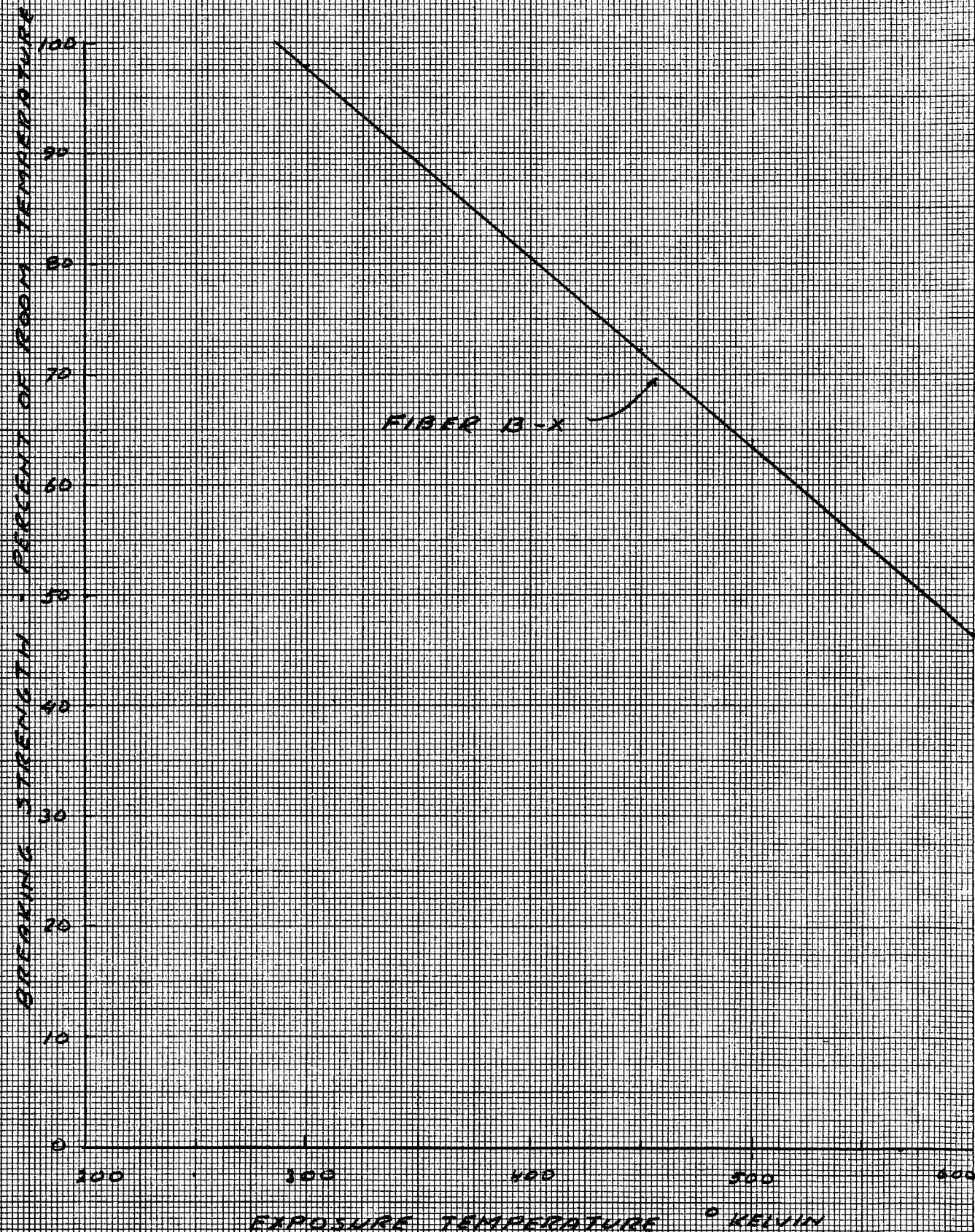
$$T_A = p R = 102,730 \times .2575$$

$$T_A = 26,400 \text{ Newtons/Meter}$$

At point B, since the circumference is smaller than at point A (Figure 17) the load per inch will be increased by the ratio of the radii  $\frac{.81468}{.6858} = 1.19$ .

$$\therefore T_B = 1.19 T_A = 1.19 \times 26,400 = 31,400 \text{ Newtons/Meter}$$

FIG 16  
EFFECT OF TEMPERATURE UPON STRENGTH  
OF DU PONT FIBER B



The G load of 4675 Newtons produces an additional load at B. Assuming that the longitudinal G load is distributed equally to both ends of the tunnel the G load will produce a fabric stress.

$$T_G = \frac{4675}{2 \times 2\pi R} = \frac{4675}{4\pi \times .685} = 543 \text{ Newtons/Meter.}$$

$$\text{Total fabric tension} = T_B + T_G = 31,400 + 543 = 31,943 \text{ Newton's/Meter}$$

Since the fabric will be folded and pleated at point B it will lose some of its efficiency. Therefore, an efficiency of 75% will be assumed.

The required fabric strength, allowing for the effect of the temperature and loss in efficiency, is

$$T = 31,943 \times \frac{4}{3} \times \frac{1}{0.88} \times 5 = 241,000 \text{ Newtons/Meter}$$

$$\text{M.S.} = \frac{262,500}{241,000} - 1 = 0.11$$

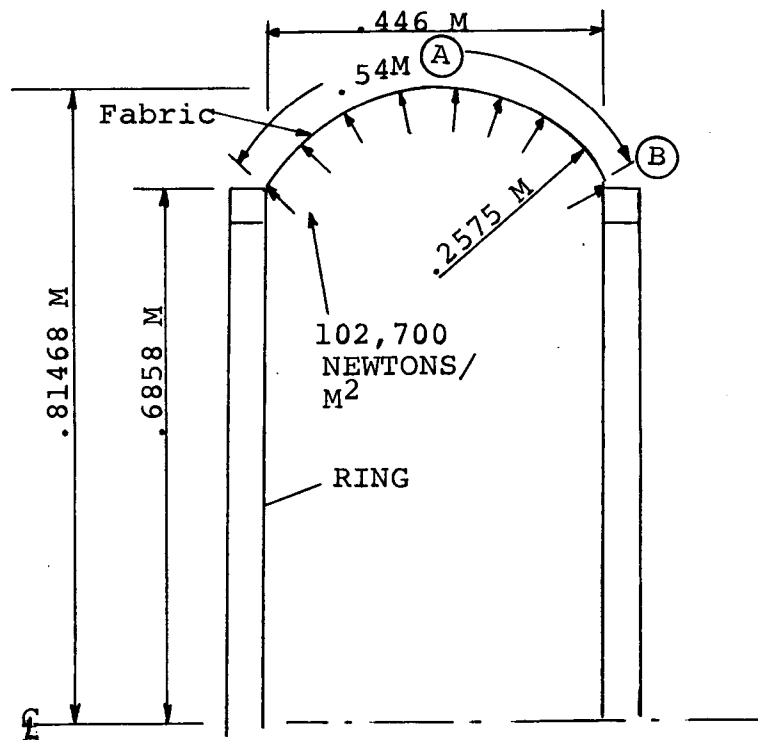


Figure 17

#### E. DEPLOYMENT AND RETRACTION LOADS

A deployment and retraction force of 1500 Newtons should be assumed for the present. There is little test data or analysis to substantiate this value. For a more accurate estimate further model and material tests will be required.

## REFERENCES

1. Technical Report AFAPL-TR-72-72, September 1972, Expandable Airlock Experiment (DO21) and the Skylab Mission (GAC Report GER-15607).
2. NASA TM X-64627, "Space and Planetary Environment Criteria Guidelines for Use in Space Vehicle Development, 1971 Revision," Aero-Astroynamics Laboratory, George C. Marshall SFC, Marshall SFC, Alabama, 15 November 1971.
3. NASA SP-8013, "Meteoroid Environment Model-1969 (Near Earth to Lunar Surface)," NASA Space Vehicle Design Criteria (Environment), NASA, March, 1969.
4. McAllum, W. E., "Development of Meteoroid Protection for Extravehicular-Activity Space Suits," Journal of Spacecraft, Vol. 6, No. 11, September, 1969, pp. 1225-1228.
5. GER-11676 S/24, "Development of Materials and Materials Application Concepts for Joint Use as Cryogenic Insulation and Micrometeoroid Bumpers," Goodyear Aerospace Corporation, June, 1966.
6. Topping, A. D., "Ring Buckling of Inflated Drag Bodies" Journal of Aircraft, Vol. 8, No. 11, November 1972.
7. Maugh, "Statically Indeterminate Structures", Wiley, 1946.
8. Anonymous, "Metallic Materials and Elements for Aerospace Vehicle Structures" MIL-HDBK-5A.
9. Anonymous, "Elastic and Thermal Properties of Roebling Aircord" John A. Roebling's Sons Corp. Report.